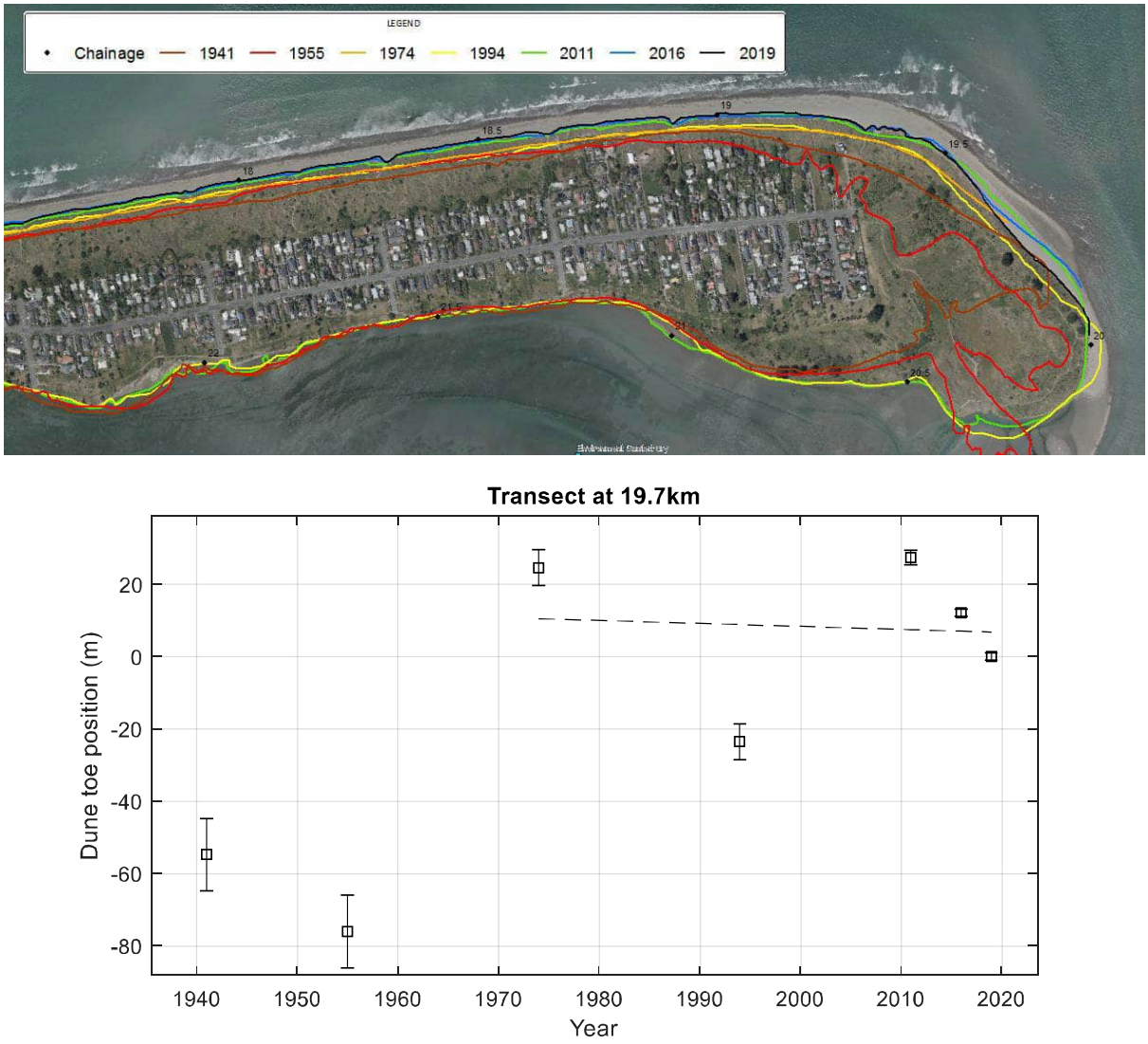

Figure 4.12: Historic shorelines and regression plot at chainage 19.7 km (distal end of Southshore Spit).

4.1.4.2 Adopted values and distribution

For this assessment a triangular distribution has been adopted for the LT component, with minimum, maximum and modal values defined within each cell. The parameter bounds have been rationalised based on the variation in the mean regression rate within each cell. For example, the upper bound is based on the maximum mean regression trend within each cell and the lower bound is based on the minimum mean regression trend within each cell. This is used in preference to a 95% confidence interval due to the often very wide range in confidence intervals due to the limited data points. LT trends within Cells 7 and 9 (seawalls) are based on the trends measured within the adjacent cells. Adopted LT parameter bounds for each cell along the Christchurch open coast are shown in Table 4.5.

Table 4.5: Adopted long-term component values for current sediment budget scenario

Cell	Long-term rate (m/yr)[1]		
	Upper	Mode	Lower
1	0.60	0	-0.60
2	0.30	0.25	0.18
3	0.30	0.25	0.18
4	0.18	0.16	0.14
5	0.12	0.08	0.00
6	0.20	0.10	-0.04
7	0.20	0.10	-0.04
8	0.20	0.10	-0.04
9	0.40	0.25	0.10
10	0.30	0.20	0.10
11	0.40	0.30	0.20
12	0.47	0.45	0.40
13	0.70	0.65	0.60
14	0.7	0.2	-0.10

[1] +ve values are accretion and -ve values are erosion.

4.1.4.3 Potential climate change effects on sediment supply

The key contributor to long-term accretion along the Christchurch open coast is the sediment supply from the Waimakariri River. Hicks et al (2018a) investigated the present day and future sediment budget for the Waimakariri River and concluded that the river contributes 182, 000 m^3/yr to the sediment budget along the Christchurch open coast shoreline, south of the river mouth.

Under future climate change conditions, the sediment supply to the Christchurch open coast may change. Based on the findings from Hicks (2018b) three future sediment supply scenarios have been assessed:

- Scenario 1: Current sediment budget. Assume current long-term rates continue.
- Scenario 2: 11% reduction in sediment supply to the coast due to climate change effects upstream.
- Scenario 3: 28% increase in sediment supply to the coast due to climate change effects upstream.

Hicks (2018b) conclude that the increase in sediment supply is a likely scenario. The long-term rates have been adjusted based on Equation 6 within Hicks (2018b)[2] (excluding the sea level rise component as this is accounted for separately within this study, see Section 0). A summary of the adjusted long-term rates accounting for the future sediment budget scenarios is shown in Table 4.6.

[2] $\Delta y = (\frac{Q_s T_e P_s}{BH} - \frac{SL}{H})$ where Q_s is the total river sand supply to the coast, T_e is the proportion of this river sand retained on the beach profile, and P_s is the proportion of the retained sand that is transported south from the river mouth to the city shore, H is the profile height above the closure point, B is the length of shoreline, S is the sea level rise and L is sum of the beach width above MSL.

Table 4.6: Adopted long-term rates (m/yr)[1] for sediment budget climate change scenarios

Cell	11% reduction in sediment supply			28% increase in sediment supply		
	Upper	Mode	Lower	Upper	Mode	Lower
1	0.48	-0.12	-0.72	0.82	0.22	-0.38
2	0.24	0.20	0.14	0.41	0.34	0.25
3	0.24	0.20	0.14	0.41	0.34	0.25
4	0.14	0.13	0.11	0.25	0.22	0.19
5	0.10	0.06	-0.02	0.16	0.11	0.02
6	0.16	0.08	-0.05	0.27	0.14	-0.03
7	0.16	0.08	-0.05	0.27	0.14	-0.03
8	0.16	0.08	-0.05	0.27	0.14	-0.03
9	0.32	0.20	0.08	0.55	0.34	0.14
10	0.24	0.16	0.08	0.41	0.27	0.14
11	0.32	0.24	0.16	0.55	0.41	0.27
12	0.38	0.36	0.32	0.64	0.62	0.55
13	0.56	0.52	0.48	0.96	0.89	0.82
14	0.56	0.16	-0.12	0.96	0.27	-0.06

[1] +ve values are accretion and -ve values are erosion.

4.1.5 Response to sea level rise (SLR)

Geometric response models propose that as sea level is raised, the equilibrium profile is moved upward and landward conserving mass and original shape. The most well-known of these geometric response models is that of Bruun (Bruun, 1962, 1988) which proposes that with increased sea level, material is eroded from the upper beach and deposited offshore to a maximum depth, termed closure depth. The increase in seabed level is equivalent to the rise in sea level and results in landward recession of the shoreline (Figure 4.13).

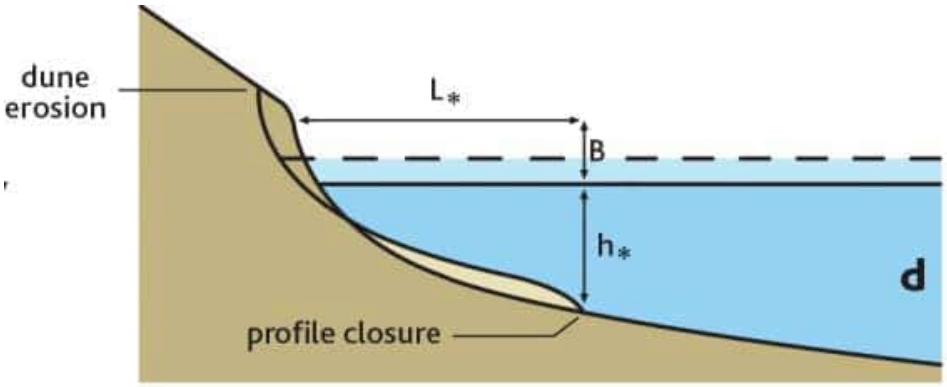

Figure 4.13: Schematic diagrams of the Bruun model for shoreline response (after Cowell and Kench, 2001).

The inner parts of the profile exposed to higher wave energy are likely to respond more rapidly to changes in sea level. For example, Komar (1999) proposes that the beach face slope is used to predict coastal erosion due to individual storms. Deeper definitions of closure including extreme wave height-based definitions (Hallermeier, 1983), sediment characteristics and profile adjustment records (Nicholls et al., 1998) are only affected during infrequent large-wave events and therefore may exhibit response-lag.

To define parameter distributions, the Bruun rule has been used to assess the landward retreat of three different active beach slope profiles (Figure 4.14):

1 Active beach face, average dune toe position to low water mark (lower bound).

2 Inner closure slope, average dune crest to inner Hallermeier closure depth (modal value).

3 Outer closure slope, average dune crest to outer Hallermeier closure depth (upper bound).

The Hallermeier closure definitions are defined as follows (Nicholls et al., 1998):

$$d_l = 2.28\, H_{s,t} - 68.5\, (H_{s,t}^2 / g T_s^2) \cong 2\, x\, H_{s,t} \quad (4.2)$$

$$d_i = 1.5\, \times\, d_l \quad (4.3)$$

Where d_l is the closure depth below mean low water spring, H_s is non-breaking significant wave height exceeded for 12 hours in a defined time period, nominally one year, and T_s is the associated period. For this study the deep water (non-breaking) wave climate parameters of H_s and T_p were based on the MetOcean wave hindcast data (1979 to 2019) from the 10 m depth contour (Table 4.7). Adopted slopes are based on average beach profiles and LINZ bathymetric contour data within each cell. A summary of the representative profiles and closure depths is presented in Table 4.8.

Table 4.7: Inner and outer profile closure depth estimates derived from Hallermeier's definitions with wave parameters sourced from the MetOcean wave hindcast

Location	Profile[1]	Significant wave height[2], $H_{s,12hr}$ (m)	Wave period[3], $T_{p,12hr}$ (s	Inner closure depth, dI (m)	Outer closure depth, di (m)
Southshore	CCC0396	2.99	7.75	7.1	10.7
Southshore	CCC0431	2.99	7.75	6.8	10.2
Brighton	CCC748	2.99	7.75	6.7	10.0
Parklands	CC1086	2.6	8.57	6.7	10.0
Waimairi	CC1273	2.6	8.57	6.7	10.0
Spencerville	CC1565	2.89	9.33	6.2	9.2
Brooklands	CC1972	2.89	9.33	6.2	9.2

[1] Average profile based on beach profile dataset. Offshore profile interpolated based on LINZ contour data.

[2] Non-breaking significant wave height exceeded for 12 hours over a year.

[3] Wave period corresponding to the non-breaking significant wave height exceeded for 12 hours over a year.

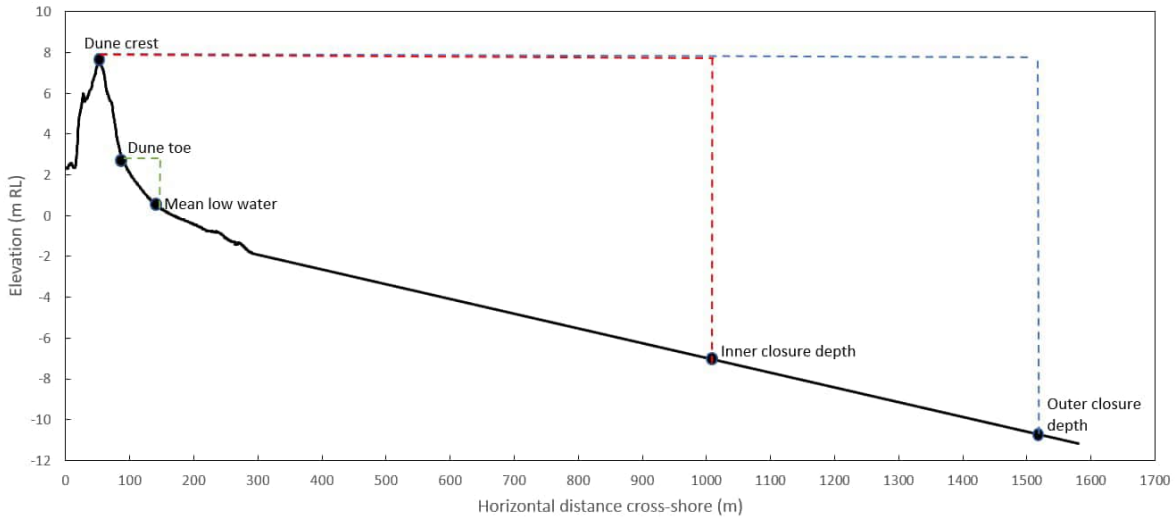

Figure 4.14: Extents of active profiles for the Christchurch Open Coast shoreline.

Table 4.8: Adopted slopes for each cell based on the profiles summarised in Table 2.7

Cells	Slope[1]		
	Lower	Mode	Upper
1 to 2	0.019	0.020	0.061
3	0.024	0.029	0.043
4 to 5	0.021	0.025	0.050
6 to 7	0.017	0.019	0.034
8	0.017	0.019	0.061
9	0.014	0.015	0.055
10	0.014	0.015	0.068
11 to 12	0.012	0.015	0.046
13 to 14	0.014	0.016	0.046

[1] Average profile based on beach profile dataset. Offshore profile interpolated based on LINZ bathymetric contour data.

4.1.6 Summary of components

Adopted component values for the Christchurch open coast are summarised in Table 4.9. Overall, the erosion susceptibility is slightly higher at the northern end of the shoreline (i.e. Cells 1 to 4) where the accretion rates are lower and the short-term storm cut potential is higher.

The assessed component values for this assessment are generally similar to the T+T (2017) assessment. The previous T+T (2017) assessment only included the open coast shoreline south of Waimairi Beach and therefore is only comparable with the updated Cells 6 to 14. For the short term component, the revised extreme value distribution is a similar shape with a slightly larger mean storm cut value compared with the previous assessment. The revised assessment includes additional data and hence there is a slight difference in values.

The long-term component is generally similar to the T+T (2017), where the average long-term rates ranged from 0.14 to 0.44 m/year. The modal values adopted in the updated assessment range from 0.1 to 0.45 m/yr through Cells 6 to 12. The updated accretion rates are slightly larger than the T+T (2017) values within Cells 13 and 14, which is likely the result of increased accretion over the recent years.

For the SLR response, T+T (2017) based the closure depths on data from the ECan wave buoy, offshore from Banks Peninsula. The adopted significant wave height was 4.2 m with a period of 10.8 s. The updated assessment has based the closure depths on the MetOcean wave hindcast data from the 10 m depth contour and subsequently the significant wave heights have been reduced, resulting in shallower closure depths and reduced closure slopes for the minimum and mode parameter bounds.

4.1.7 Uncertainties

Key uncertainties in the erosion hazard assessment along the Christchurch open coast shoreline include:

- Tidal inlet response to SLR and the subsequent effects on the long term shoreline trends at the distal end of the Southshore Spit.
- Future sediment supply from the Waimakariri River and subsequently the long term accretion rates.

Table 4.9: Adopted component values for the Christchurch open coast shoreline

Cell		1	2	3	4	5	6	7	8	9	10	11	12	13	14
Chainage, km (from Waimakariri River mouth)		0 to 1.2	1.2 to 4.5	4.5 to 7	7 to 8	8 to 10	10 to 11.7	11.7 to 12	12 to 13	13 to 13.6	13.6 to 15.1	15.1 to16.5	16.5 to 18	18 to 19	10 to 20.5
Morphology		Dune (Spit end)	Dune	Dune	Dune	Dune	Dune	Dune	Dune	Dune	Dune	Dune	Dune	Dune	Dune (Spit end)
Short-term (m)	**mu (mean)**	-11	-5.9	-5.9	-5.9	-3.6	-3.6	-3.6	-3.6	-3.6	-3.6	-3.6	-3.6	-3.6	-5.5
	sigma (shape parameter)	7	4.7	4.7	4.7	2.3	2.3	2.3	2.3	2.3	2.3	2.3	2.3	2.3	1.86
Dune (m above toe)	**Lower**	1	4	3.5	3	4.5	4	0.5	4	1	4	3	2.5	1.8	2
	Mode	2	5	4	4	5.5	5	0.8	5	1.5	5	3.5	3	2	3
	Upper	3	7.5	5	5	6.5	7	1	6	2	6	4.5	5	3	4
Stable angle (deg)	**Lower**	30	30	30	30	30	30	30	30	30	30	30	30	30	30
	Mode	32	32	32	32	32	32	32	32	32	32	32	32	32	32
	Upper	34	34	34	34	34	34	34	34	34	34	34	34	34	34
Long-term (m) -ve erosion +ve accretion	**Lower**	0.6	0.30	0.30	0.18	0.12	0.20	0.20	0.20	0.40	0.30	0.40	0.47	0.70	0.7
	Mode	0	0.25	0.25	0.16	0.08	0.10	0.10	0.10	0.25	0.20	0.30	0.45	0.65	0.2
	Upper	-0.6	0.18	0.18	0.14	0.00	-0.04	-0.04	-0.04	0.10	0.10	0.20	0.40	0.60	-0.1
Closure slope	**Lower**	0.060	0.060	0.040	0.050	0.050	0.030	0.030	0.06	0.06	0.07	0.05	0.05	0.05	0.050
	Mode	0.020	0.020	0.029	0.025	0.025	0.019	0.019	0.019	0.015	0.015	0.015	0.015	0.016	0.016
	Upper	0.019	0.019	0.024	0.021	0.021	0.017	0.017	0.017	0.014	0.014	0.012	0.012	0.014	0.014

4.2 Sumner

Sumner beach is a northeast facing shoreline located at the southern extent of Pegasus Bay. The northern end of the shoreline is influenced by the Avon-Heathcote estuary inlet while the southern end is bound by Sumner Headland. Cave Rock is a basalt outcrop that extends into the sea and acts as a natural groyne blocking some of the sediment transport into Sumner Bay on the eastern side. On the western side of Cave Rock is Clifton Beach which is largely influenced by dynamics of the Avon-Heathcote estuary inlet-delta system. Sumner settlement has been well established since 1880 and there has since been shoreline modifications with numerous seawalls constructed.

4.2.1 Cell splits

The shoreline has been split into three coastal cells (Figure 4.15). Cell 27 is within Clifton Bay at the eastern edge of the Avon-Heathcote estuary inlet. The beach shoreline is protected by a rock revetment. Cell 28 is an unprotected beach shoreline within Clifton Bay, on the north-western side of Cave Rock. Both Cells 27 and 29 have been classified as Class 1 structures (Figure 4.16) (refer to Section 3.1.5).

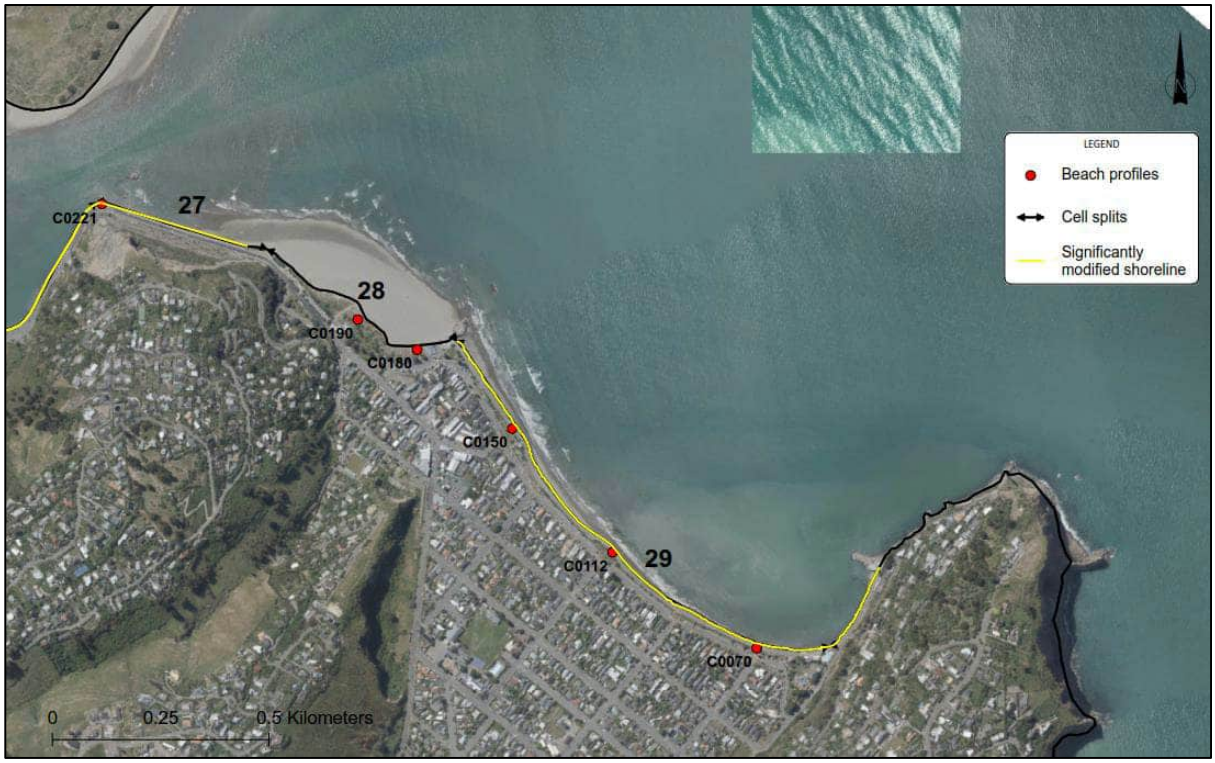

Figure 4.15: Overview of cell splits along the Sumner shoreline.

4.2.2 Short term component (ST)

There are six beach profiles along the Sumner shoreline, one of them is in front of the revetment near Shag Rock, two of them are along the natural dune within Clifton Bay and three of them are along the revetment within Sumner Bay.

For the areas with Class 1 structures, the current hazard is defined as the immediate hazard if the structure were to fail. This is assessed based on the structure height and stable angle of repose (see Section 4.2.3.

The short-term component along Clifton Beach been assessed using the same beach profile analysis method as adopted for the Christchurch open coast (Section 4.1.2). Figure 4.17 shows profile

CCC0190 within Cell 28 and the regression analysis at the 2.5 m RL contour. While the beach width seaward of the dune tends to show large fluctuations (up to 100 m) in response to changes in the inlet delta, the dune toe (2.5 m RL contour) shows relatively small fluctuations (up to 6 m). It is likely that the wide beach provides a buffer against significant storm cut along the dune toe.

Figure 4.16: Site photos (taken August 2020) for the Sumner shoreline. (Left) unprotected dunes along Clifton Beach (Cell 28), (right) rock revetment along Sumner Bay with Sumner Headland in the background (Cell 29).

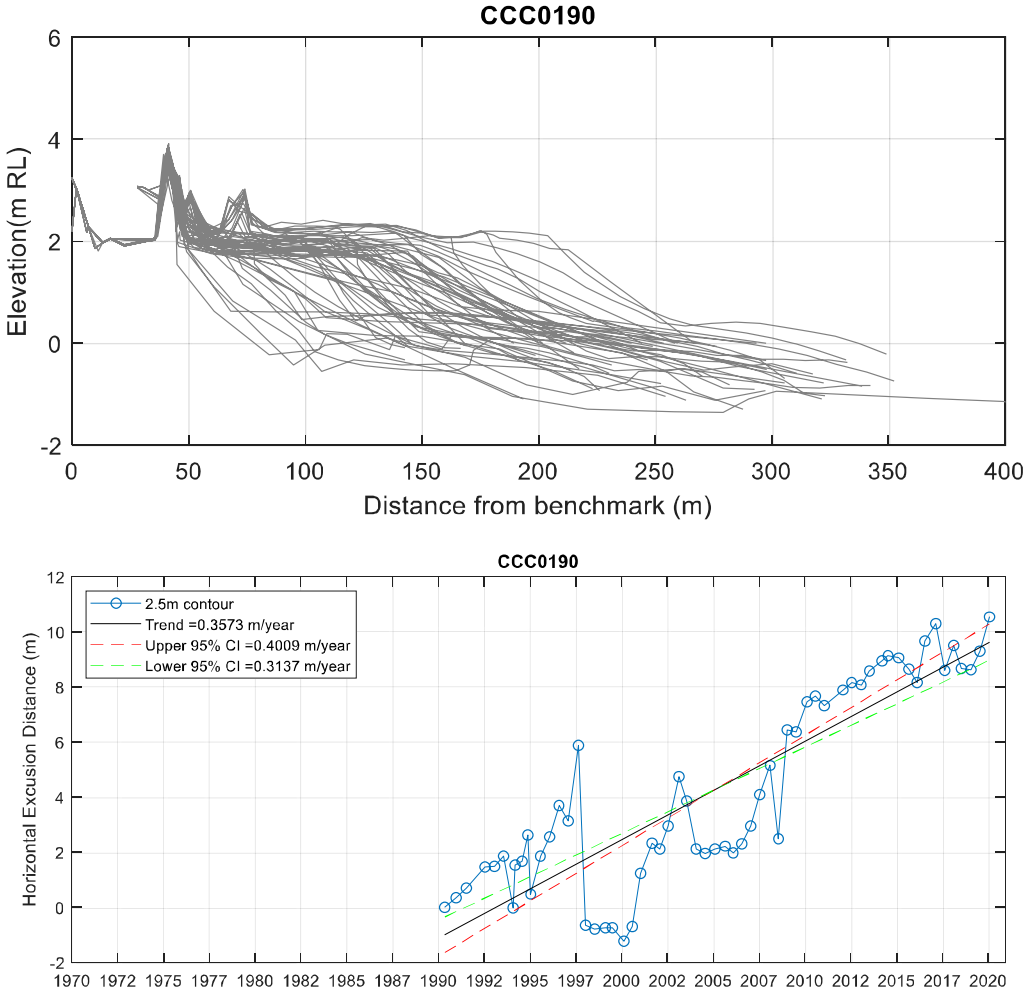

Figure 4.17: Beach profiles and regression plot for profile CCC0190 within Cell 28, Sumner.

As with the Christchurch open coast, the measured inter-survey storm cut distances have been assessed using an Extreme Value Analysis (EVA). Extreme value distributions for profile CC0190 (Cell 28) are shown in Figure 4.18. The mean storm cut at the 2.5 m RL contour Cell 28 is less than 1 m (Table 4.10).

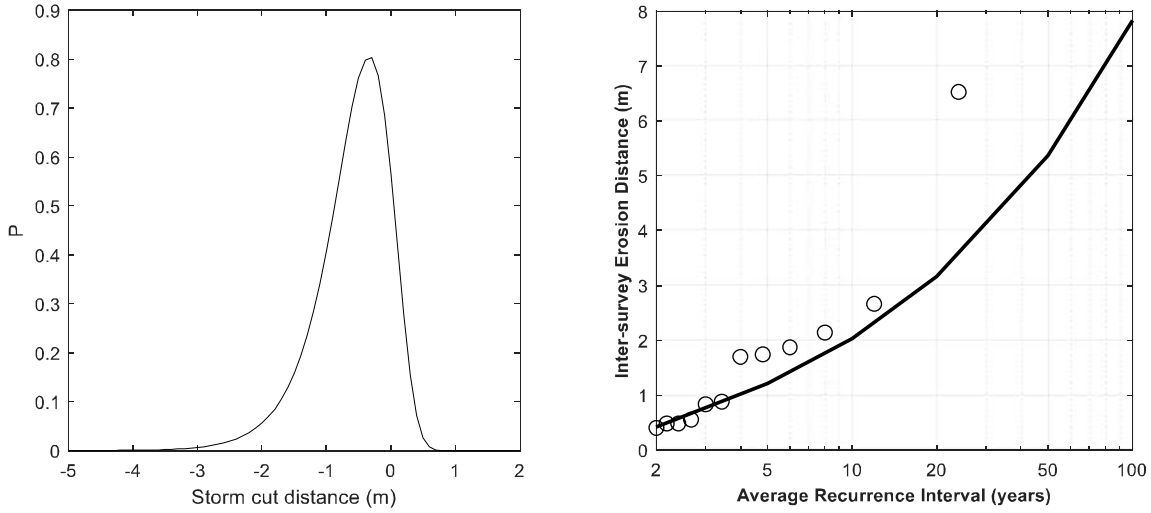

Figure 4.18: Example of extreme value distribution and curve for inter-survey storm cut distances at Clifton Beach (profile CC00190).

Table 4.10: Summary of extreme value distributions for inter-survey storm cut distances along Clifton Beach

Cell	Mean inter-survey storm cut (μ) (m)	Shape parameter (σ)[1]	Resultant 100 year ARI storm cut (m)
28	-0.34	0.5	-8

[1] Shape parameter describes the shape of the distribution (e.g., a larger shape parameter results in a wider distribution).

4.2.3 Dune stability (DS)

Dune stability for the Sumner coast has been assessed as described in Section 4.1.3. Parameter bounds are defined based on the variation in dune/structure height within the coastal cell and potential range in stable angle of repose (Table 4.11 and Table 4.12). The stable angle of repose for Cell 28 is based on the angle of repose for dune sand, while the stable angle of repose within Cells 27 and 29 is based on an assumed angle of repose for fill material behind the structure.

Table 4.11: Dune stability component values for Sumner Beach

Cells	Dune stability component values		
	Lower (degrees)	Mode (degrees)	Upper (degrees)
27	18	22	26.6
28	30	32	34
29	18	22	26.6

Table 4.12: Dune and structure height component values

Cell	Dune/structure height component values		
	Lower (m)	Mode (m)	Upper (m)
27[1]	2.5	2.8	3
28	0.5	1	2
29[1]	1	2	3

[1] Height of Class 1 structure.

4.2.4 Long-term component (LT)

It is apparent that Clifton Beach (Cell 28) has undergone periods of erosion and accretion which generally are related to changes in the adjacent inlet delta. Thompson (1994) found that periods of erosion at Southshore tend to correspond to accretion at Clifton Beach and *vice versa*. Findlay and Kirk (1988) state the main ebb channel from the estuary historically flowed south-east past Shag Rock and changed to its current position during 1938. The change in channel position is likely to have contributed to the extensive infilling of Clifton Beach between 1927 and 1950s.

Historical shoreline data (from aerial imagery) indicates Clifton Beach (Cell 28) has experienced long-term accretion, with up to 20 m accretion since the 1940s (Figure 4.19). The beach profile data also shows some fluctuations with overall accretion at the 2.5 m RL contour at an average rate of 0.36 m/year (Figure 4.17).

Hicks et al (2018a) noted that the phase of accretion since 2011 may be associated with effects from the earthquakes. Following the earthquake there was a reduction in the tidal prism and subsequently a reduced volume on both the ebb and flood tidal deltas at the inlet entrance. This reduction in delta size has potentially resulted in a surplus of sand being supplied to the adjacent shoreline and hence the period of accretion following 2011 (Figure 4.17).

As with the distal end of the Southshore Spit, there is high uncertainty in future erosion rates along the shoreline adjacent to the tidal inlet (see Section 4.1.4). SLR may result in an increased tidal prism within the Avon-Heathcote Estuary which would lead to widening of the tidal inlet and increased erosion along the adjacent shoreline. Quantification of this is, however, beyond the scope of this assessment.

Long-term rates adopted for the Clifton Beach are summarised in Table 4.13.

Figure 4.19: Historical shorelines along Clifton Beach.

Table 4.13: Adopted long-term component values for Sumner beach

Cell	Long-term rate (m/yr)[1]		
	Upper	Mode	Lower
28	0.4	0.2	0.1

[1] +ve values are accretion and -ve values are erosion.

4.2.5 Response to sea level rise (SLR)

The shoreline response to sea level rise has been assessed based on the Bruun model described in Section 0. Wave climate parameters and resultant closure depths are summarised in Table 4.14.

Table 4.14: Inner and outer profile closure depth estimates derived from Hallermeier's definitions with wave parameters sourced from the MetOcean wave hindcast

Cell	Significant wave height, $H_{s,12h}$ (m)	Wave period, $T_{p,12h}$ (s)	Inner closure depth, dI (m)	Outer closure depth, di (m)	Slope		
					Lower	Mode	Upper
28	3.01	10.06	7.11	10.67	0.014	0.016	0.014

4.2.6 Summary of components

Adopted component values for the Sumner shoreline are summarised in Table 4.15.

4.2.7 Uncertainties

Key uncertainties in the erosion hazard assessment along the Sumner shoreline include:

- Condition and design life of structures along the 'significantly modified shoreline'.
- Tidal inlet response to SLR and the subsequent effects on the long term trends along the adjacent shoreline at Clifton Beach.

Table 4.15: Adopted component values for the Sumner shoreline

Cell		**27**	**28**	**29**
Chainage, km from Waimakariri River mouth		35.6 to 36	36 to 36.6	36.6 to 37.8
Morphology		Class 1 structure	Dune	Class 1 structure
Geology		Anthropic deposits	Dune deposit	Anthropic deposits
Short-term (m)	mu (mean)	N/A	-0.34	N/A
	sigma (shape parameter)		0.5	
Dune (m above toe)	Lower	2.5	0.5	1
	Mode	2.8	1	2
	Upper	3.0	2	3
Stable angle (deg)	Lower	18	30	18
	Mode	22	32	22
	Upper	26.6	34	26.6
Long-term (m) -ve erosion +ve accretion	Lower	N/A	0.4	N/A
	Mode		0.2	
	Upper		0.1	
Closure slope	Lower		0.014	
	Mode		0.016	
	Upper		0.046	

4.3 Taylors Mistake

Taylors Mistake/Te Onepoto is a small, northeast-facing, pocket beach on the southern side of Sumner Head. The embayment is bound by volcanic cliffs on either side. The beach comprises fine sand with a relatively flat profile (approximately 1(V):20(H)). The beach at the northern end includes a slightly narrower dune with the surf club and at the southern end there is a wider dune system that has infilled a historical stream channel/lagoon (Figure 4.20). There is still an ephemeral stream channel which discharges onto the coast under high rainfall events.

Figure 4.20: Site photos (taken August 2020) along Taylors Mistake. (Top left) Oblique photo of southern end of shoreline (top right) fencing along dunes at northern end of shoreline, (bottom left) southern end of beach, (bottom right) historical stream mouth.

4.3.1 Cell splits

Taylors Mistake beach has been classified into one coastal cell, approximately 350 m long (Figure 4.21).

Figure 4.21: Overview of cell extent along the Taylors Mistake shoreline.

4.3.2 Short term component

For Taylors Mistake, the majority of the beach has natural dunes and therefore, the short-term component has been assessed based on the same approach as the Christchurch open coast, using the inter-survey horizontal excursion distance of the dune toe, measured from beach profiles (see Section 4.1.2).

Extreme Value Analysis (EVA) has been completed based on the measured inter-survey storm cut distances at each beach profile. The distribution from profile BPN8010 has been adopted as shown in Figure 4.22. The adopted extreme value distribution (mean and shape parameter values) for Taylors Mistake are summarised in Table 4.16. The 100 year ARI storm cut distance is also included for context.

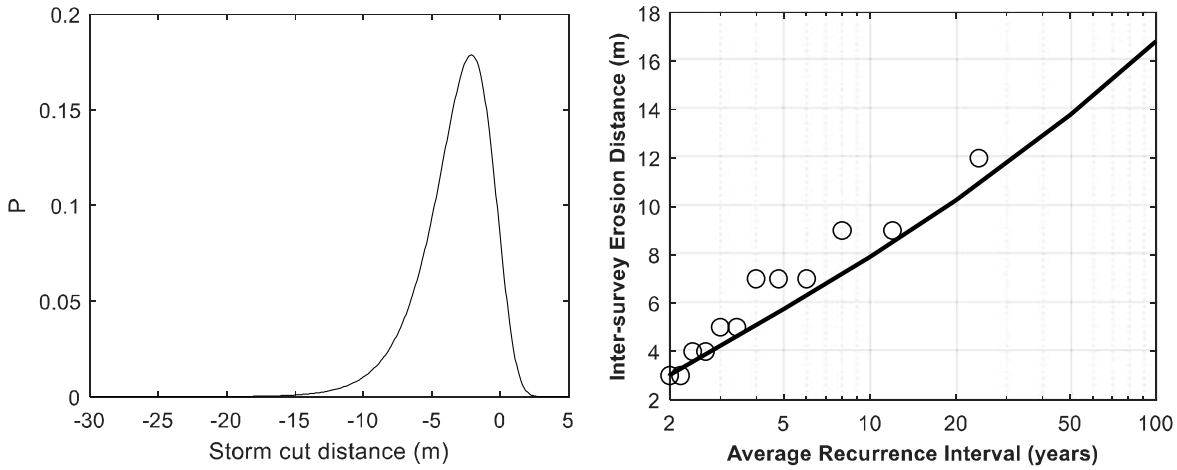

Figure 4.22: Extreme value distribution for inter-survey storm cut distances along Taylors Mistake.

Table 4.16: Summary of extreme value distributions for inter-survey storm cut distances at Taylors Mistake

Cell	Mean inter-survey storm cut (μ) (m)	Shape parameter (σ)[1]	Resultant 100 year ARI storm cut (m)
30	-6.5	1.8	-17

[1] Shape parameter describes the shape of the distribution (e.g., a larger shape parameter results in a wider distribution).

4.3.3 Dune stability (DS)

Dune stability for the Taylors Mistake has been assessed as described in Section 4.1.3. Parameter bounds are defined based on the variation in dune height within the coastal cell and potential range in stable angle of repose (Table 4.17 and Table 4.18).

Table 4.17: Dune stability component values for Taylors Mistake

Cell	Dune stability component values		
	Lower (degrees)	Mode (degrees)	Upper (degrees)
30	30	32	34

Table 4.18: Dune height component values for Taylors Mistake

Cell	Dune height component values		
	Lower (m)	Mode (m)	Upper (m)
30	0.8	1.1	1.5

4.3.4 Long-term trends (LT)

The long-term trends have been assessed based on historical shoreline data and beach profiles (Figure 4.23 and Figure 4.24). The beach profiles show that majority of the beach has been relatively stable with a slight erosion trend, except at profile BPN7975, at the southernmost end where there has been an accretion trend (Figure 4.23). The accretion trend at BPN7975 is not likely to be representative of the remainder of the beach as it is influenced partially be the stream and infilling that has occurred. The historical shorelines show that the southern end has infilled since at least 1974, with some fluctuations due to the ephemeral stream which discharges onto the coast under high rainfall events (Figure 4.23 and Figure 4.25).

Overall, since 1990 the beach has generally shown a slight erosion trend, ranging from -0.04 m/yr to -0.23 m/yr (Figure 4.23). Based on changes in historic shorelines from aerial photographs, and variation in mean regression rates measured from the beach profile data, the adopted long-term rates range from 0.2 m/year to -0.2 m/year (Table 4.19).

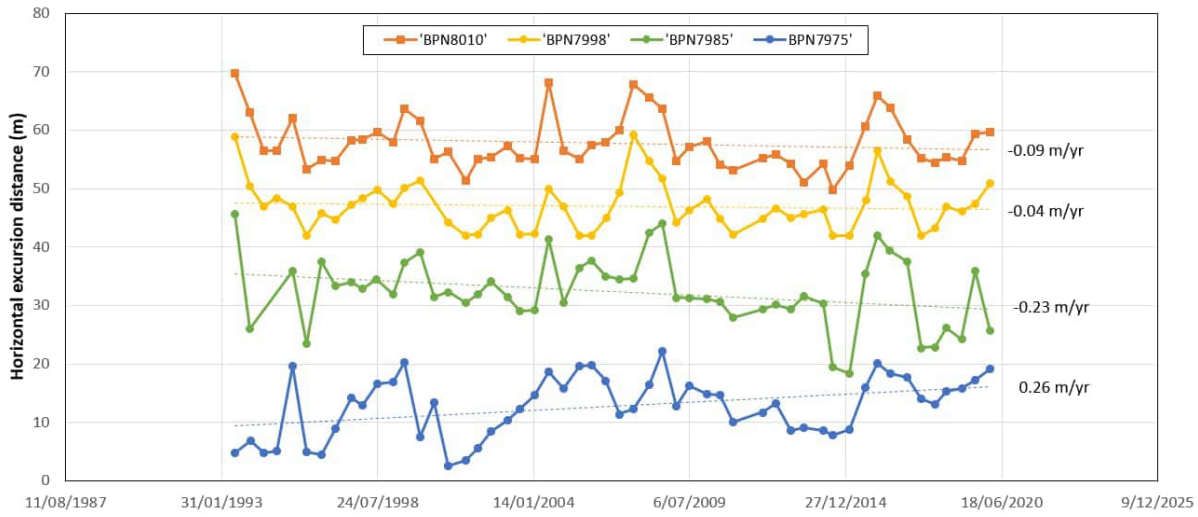

Figure 4.23: Regression analysis of beach profiles along Taylors Mistake.

Figure 4.24: Historic shorelines for Taylors Mistake.

Figure 4.25: Google Earth photos showing the ephemeral stream discharging onto the beach in September 2010, infilling by February 2016 and again discharging during August 2019.

Table 4.19: Adopted long-term rates along Taylors Mistake

Cell	Long-term rate (m/yr)		
	Lower	Mode	Upper
30	-0.2	-0.05	0.2

NOTE: Positive values are accretion and negative values are erosion.

4.3.5 Response to sea level rise (SLR)

The shoreline response to sea level rise has been assessed based on the Bruun model described in Section 0. Wave climate parameters and resultant closure depths are summarised in Table 4.20

Table 4.20: Inner and outer profile closure depth estimates derived from Hallermeier's definitions with wave parameters sourced from the MetOcean wave hindcast

Cell	Profile	Significant wave height, $H_{s,\ 12hr}$ (m)	Wave period, $T_{p,\ 12hr}$ (s)	Inner closure depth, dI (m)	Outer closure depth, di (m)	Slope[1]		
						Lower	Mode	Upper
30	BPN7998	3.02	8.12	6.8	10.2	0.016	0.017	0.076

[1] Average profile based on beach profile dataset. Offshore profile interpolated based on LINZ contour data.

4.3.6 Summary of components

Adopted component values for Taylors Mistake are summarised in Table 4.21.

4.3.7 Uncertainties

Key uncertainties in the erosion hazard assessment for the Taylors Mistake shoreline include:

- The influence of the ephemeral stream on short-term storm cut and long term trends.
- Future sediment supply and subsequently the long term accretion rates.

Table 4.21: Adopted component values for Taylors Mistake

Cell		30
Chainage, km from Waimakariri River mouth		40.6 to 41.1
Morphology		Dune
Geology		Dune deposit
Short-term (m)	mu (mean)	-6.5
	sigma (shape parameter)	1.8
Dune (m above toe)	Lower	0.8
	Mode	1.1
	Upper	1.5
Stable angle (deg)	Lower	30
	Mode	32
	Upper	34
Long-term (m) -ve erosion +ve accretion	Lower	-0.2
	Mode	-0.05
	Upper	0.2
Closure slope	Lower	0.016
	Mode	0.017
	Upper	0.076

4.4 Avon-Heathcote estuary

The Avon-Heathcote Estuary is a shallow intertidal estuary on the eastern side of Christchurch City. The Avon River flows into the northeastern corner and the Heathcote River into the southwestern corner. Their combined catchments give the estuary a total catchment area of 200 km^2 (MacPherson, 1978).

The estuary has a short inlet connection with the sea at the southern end and is partially enclosed by the 4 km long Southshore Spit. The estuary is on a coastal plain which consists of Late Quaternary terrestrial and estuarine gravels, sands, peats and mud. At the southern margin is the volcanic rock of Banks Peninsula. The suburbs which boarder the western side of the estuary were extensive swamplands until European settlement in the 1850s. The estuary has naturally infilled over time however early urbanisation led to a rapid increase of fine sediment to the estuary, particularly between 1850 and 1875 (MacPherson, 1978).

The southern margin of the estuary has undergone significant modification with construction of sea walls, causeways and reclamation. Historically, there was a vegetated flat island (Skylark Island) off the eastern end of McCormacks Bay. Erosion of the island began immediately after construction of the McCormacks Bay causeway in 1907 and by 1920 the island was reduced to mudflats (Findlay, 1988). Other modifications include the construction of various public and private seawalls along Southshore, Main Road, Beachville Road and Humphreys Drive. Findlay (1988) state the Beachville Road seawall was constructed in 1933.

4.4.1 Cell splits

The Avon-Heathcote estuary has been split into 12 cells (Figure 4.26). The eastern margin of the estuary is characterised by low-lying, unconsolidated shoreline with ad-hoc structures along sections (Figure 4.27). Sections of the shoreline, particularly at the northern end (i.e., Cell 20) are fronted with salt marsh vegetation. The western margin is characterised by unconsolidated estuary deposits and includes the Bromley oxidation ponds which comprise anthropic fill material along the shoreline. The southern end of the estuary (Cells 25 and 26) is classified as ‘significantly modified shoreline’ (see Section 3.1.5), comprising the causeway, some reclamation and various protection structures since the early 1900’s (Figure 4.27).

Figure 4.26: Overview of cell extents around the Avon-Heathcote estuary shoreline.

Figure 4.27: Site photos (taken August 2020) around the Avon-Heathcote estuary shoreline. (Top left) natural unconsolidated shoreline on the western side of Southshore spit (Cell 15), (top right) rip rap along the unconsolidated shoreline near Penguin Street (Cell 17), (centre left) eroded shoreline near South New Brighton Park (Cell 19), (centre right) gravel shoreline near Windsurfer's Reserve (cell 24), (bottom left) protected bank near Humphreys Drive (Cell 25), (bottom right) protected bank near Beachville Road (Cell 26).

4.4.2 Short term component (ST)

The short term storm cut component along the estuary shoreline has been assessed based on the convolution method developed by Kriebel & Dean (1993). The method considers beach profile equilibrium response to storm events. The method includes initial beach geometry, peak nearshore water level and breaking wave height to determine the maximum potential erosion that would be achieved if the beach could respond to equilibrium (Figure 4.28 and Equation 4.4). Due to the method using equilibrium profiles the storm cut distances are conservative as it is not restricted to the storm event duration. However, as resulting storm cut distances are relatively small, the approach is considered acceptable.

$$R_{\infty} = \frac{S(x_b - \frac{h_b}{m})}{B + h_b - \frac{S}{2}} \quad (4.4)$$

Where:

S = Water level rise.

X_b = Distance to breaking location.

h_b = Breaking depth.

m = (Linear) beach slope.

B = Berm height above the initial water level.

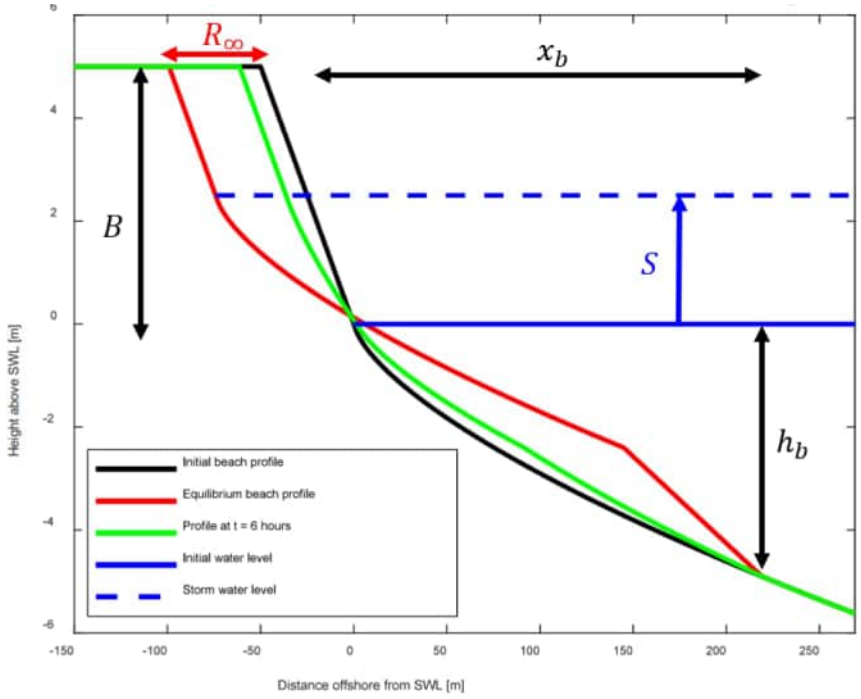

Figure 4.28: Schematic showing the beach storm response based on Kriebel and Dean (1993).

The short term storm cut has been assessed for a range of different storm tide levels and wave heights (Table 4.22). Assessed storm tide levels are based on the 1 year, 10 year and 100 year ARI water levels from the Bridge Street tide gauge. Wave heights are based on the wave height range simulated in the SWAN model (see Appendix A). Based on the LiDAR data a representative profile with an assumed berm elevation of 1.5 m NZVD-16 and an upper slope of 5(H):1(V) has been adopted for assessing the short term along the unconsolidated shoreline within the Avon-Heathcote estuary. Results indicate the short-term component ranges from 1 to 5 m (Table 4.22 and Figure 4.29).

Table 4.22: Summary of storm tide and wave heights used to assess storm cut along the estuary shoreline

	Storm tide level (m NZVD)[1]	Breaking wave height[2] (m)	Storm cut (m)
Lower bound	1.33	0.4	1
Mode	1.59	0.6	3
Upper bound	1.89	0.8	5

[1] Based on 1 year, 10 year and 100 year storm tide levels within the Avon-Heathcote estuary.

[2] Based on SWAN model outputs, for the average 1 year, 10 year and 100 year ARI wind speeds see Appendix B).

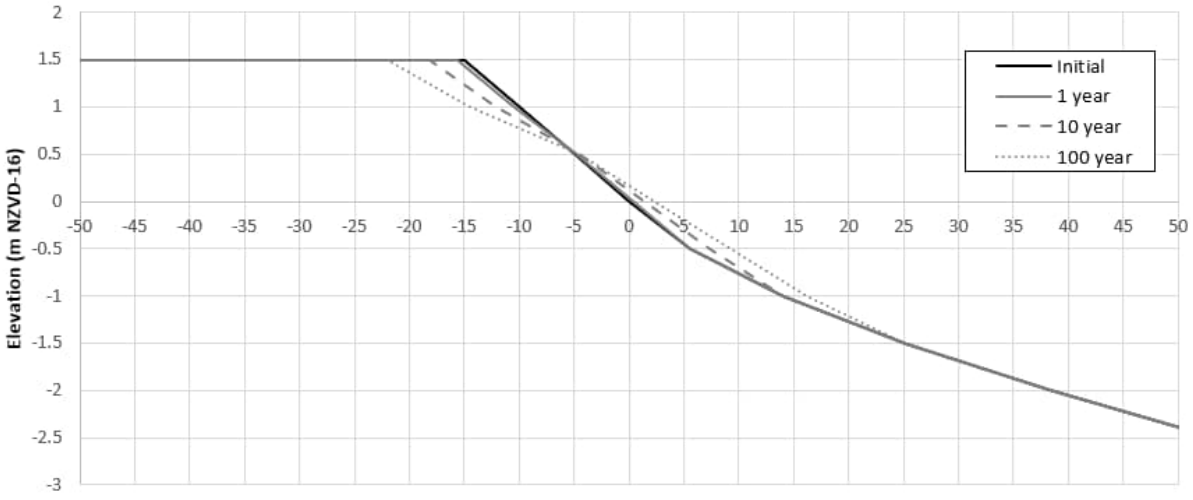

Figure 4.29: Example of beach response for the estuary shoreline under different storm conditions.

4.4.3 Long-term trends (LT)

The long-term component has been assessed based on regression analysis of historic shorelines derived from aerial photographs. Due to tree coverage and marsh vegetation, it is difficult to accurately identify the shoreline position along the entire site, particularly in the earlier historic aerials. Subsequently, the long-term trends have been assessed along several representative transects around the estuary (Figure 4.30).

Figure 4.30: Location of transects used to assess the long term trends around the Avon-Heathcote estuary.

4.4.3.1 Impact of the 2011 Canterbury Earthquakes

The effect of the 2011 Canterbury earthquake sequence (CES) has been considered. There are areas where there has been significant erosion of estuary vegetation due to land subsidence following the quakes. The significant loss of vegetation is not likely to be indicative of the long-term trends but instead shows the instantaneous response to subsidence. Therefore, long term rates have been based on the pre-quake trends.

Figure 4.31 provides an example along the Southshore shoreline where there has been increased shoreline erosion following the quake. The long-term trend pre-quake was -0.16 m/yr while the long-term including the earthquake induced erosion is -0.22 m/yr. Cells 16 to 24 typically show an increased erosion rate including post-quake (i.e. 1941 to 2020) compared with pre-quake (i.e. 1941 to 2011) (Table 4.23). It is uncertain whether the increased erosion rate will continue or whether the shoreline has reached an equilibrium state.

There is also uncertainty in how the areas of shoreline where there is salt marsh will adjust once the salt marsh vegetation is eroded away. It is possible that the shoreline landward of the salt marsh will erode at a slower rate compared to the erosion rate measured for the salt marsh vegetation.

However, in some areas the loss of vegetation may increase the shoreline exposure and subsequently the erosion rate.

Based on these uncertainties adopted long-term rates are based on the pre-quake trends and the transects less influenced by salt marsh vegetation (i.e. AH5). Adopted parameter bounds for long term component within each cell around the Avon-Heathcote estuary are presented in Table 4.24.

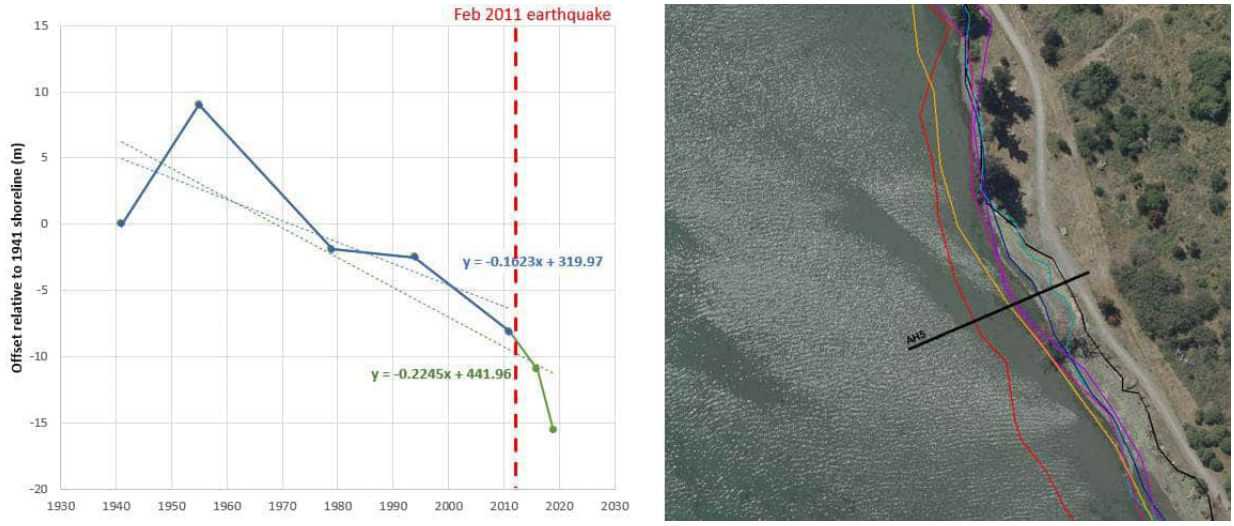

Figure 4.31: Example of long-term trends assessed using historic shoreline data within the Avon Heathcote Estuary. Profile is AH5 within Cell 19.

Table 4.23: Summary of regression rates measured from aerial imagery along each transect

Cell	Transect	Average regression rate (m/yr)[1,2]	
		1941 to 2020	1941 to 2011 (pre-quake)
15	AH1	+0.37	+0.44
	AH1a	+0.14	+0.17
16	AH2	+0.08	+0.07
17	AH3	-0.34	-0.17
	AH4	-0.45	-0.40
	AH4a	-0.12	-0.16
19	AH5	-0.22	-0.16
	AH5a	-0.08	-0.07
20	AH6	-0.18	-0.18
21	AH7	-0.30	-0.03
	AH8	-0.15	-0.11
23	AH9	-0.13	-0.13
24	AH10	-0.01	0

[1] +ve values are accretion and -ve values are erosion.

[2] Long-term rates for AH2 to AH5 are potentially influenced by shoreline protection works.

4.4.4 Dune/bank stability (DS)

Dune and bank stability around the Avon-Heathcote estuary has been assessed as described in Section 4.1.3. Parameter bounds are defined based on the variation in dune/bank height within the coastal cell and potential range in stable angle of repose. Adopted dune/bank heights and stable angles are shown in Table 4.24.

4.4.5 Response to sea level rise (SLR)

The estuary shoreline typically comprises either silty sand, fine sand, shell or mixed sand and gravel on the upper beach face with a wide intertidal zone and no extensive dune system. Due to this variation between the composition of the upper beach and the intertidal flats, the estuary shoreline is expected to behave differently to sandy beaches in response to a rise in mean sea level. The effect of sea level rise on estuarine type shorelines can be highly variable and complex and will depend on the interrelationship between:

- Backshore topography and geology.
- Sediment supply and storage.
- The wave energy acting on the shoreline.

While estuaries tend to be areas of sediment deposition, it is expected that future sea level rise will be greater than the rate of sedimentation and therefore there will be an increase in water depth across the estuary. The greater water depth will allow greater wave heights to act on the shoreline and subsequently increase the erosion potential. However, as it is a lower energy environment, erosion is likely to occur more episodically and more slowly than a more energetic open coast environment.

The traditional Bruun Rule, developed for open coast uniform sandy beaches that extend down beyond where waves can influence the seabed, does not directly apply for estuarine beaches where the upper beach is a markedly different composition from the intertidal areas. However, a modified equilibrium beach concept that assumes that the upper beach profile is likely to respond to increasing sea level rise with an upward and landward translation over time was accepted by the peer review panel (Kenderdine et al., 2016) as appropriate in this setting and was applied for harbour environments by T+T (2017). The landward translation of the beach profile (SL) can be defined as a function of sea level rise (SLR) and the upper beach slope (tanα). The upper beach slope above the intersection of the beach and the fronting intertidal flats has been adopted for each cell. The equilibrium profile method relationship is given in Equation 4.5.

$$SL = \frac{SLR}{\tan \alpha} \quad (4.5)$$

Where:

SLR = Increase in sea level rise (m) for the areas where the present height of beach above MHWS is higher than projected sea level rise increase; or the height of the beach above MHWS where the beach is lower than the sea level rise value.

tanα = Average slope of the upper beach.

In low energy environments there is likely to be insufficient energy to reform the beach crest to match the increase in sea level and subsequently once sea levels exceed the crest, inundation becomes the more significant controlling factor. Therefore, the maximum potential extent of SLR induced erosion for low-lying beach areas is assumed to be controlled by the crest height above the MHWS. Where the beach crest is higher than the projected sea level rise, the sea level value has been used. This means that when sea level exceeds the crest height and inundation occurs, there is

no additional increase in erosion of the present-day shoreline. This method approximately follows the method by Komar et al. (1999), with the MHWS adopted as the dune-toe level.

The land subsidence that occurred during and following the 2011 earthquake provides an example of instantaneous sea level rise and the subsequently shoreline response. Figure 4.32 shows a cross-section along the South Brighton shoreline where the beach face slope is approximately 10%. Between February 2011 and December 2011, the LiDAR indicates the land subsided by approximately 0.25 m which is in line with the findings from Orchard (2020). The subsidence was equivalent to 0.25 m SLR and based on the LiDAR resulted in approximately a 2.5 m landward shift in shoreline position (Figure 4.32). This example of instantaneous SLR demonstrates that Equation 3-5 is appropriate for estimating the estuary shoreline response to future SLR. The adopted upper beach slopes for cells around the Avon-Heathcote estuary are shown in Table 4.24.

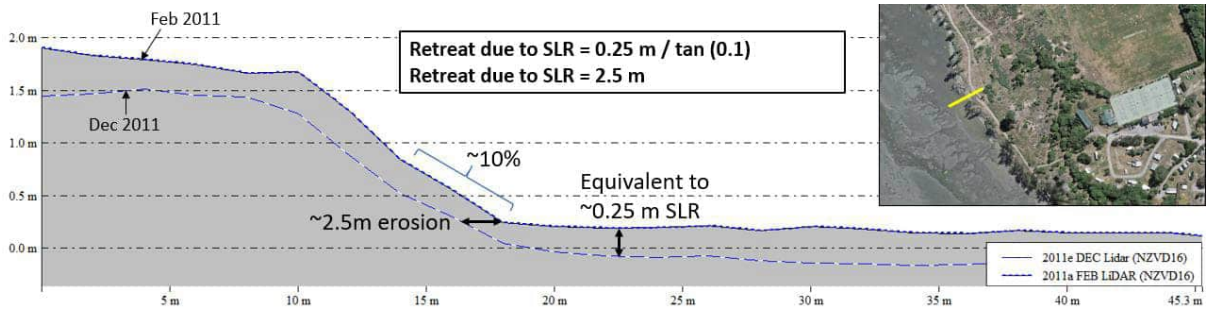

Figure 4.32: Example of shoreline response to SLR within the Avon-Heathcote Estuary.

4.4.6 Summary of components

Adopted component values for the Avon-Heathcote estuary are shown in Table 4.24.

4.4.7 Uncertainties

Key uncertainties in the erosion hazard assessment for the Avon-Heathcote estuary include:

- Long term erosion rates in absence of the protection structures, particularly along the southern margin.
- Long-term rates following the CES. Adopted rates are based on the pre-quake rates which could be non-conservative.
- Condition and design life of structures along the 'significantly modified shoreline'.
- Short term storm response. The Kriebel and Dean (1993) method does not account for different sediment types across the profile or response to short-duration events.
- Shoreline response to SLR. Estuaries are areas of deposition and infilling so if sedimentation rates are high, the shoreline may adjust and keep pace, depending on the rate of SLR.
- The effect of modified hydrodynamics and sediment transport regimes due to changed bed levels following the earthquake.

Table 4.24: Summary of adopted component values for the Avon-Heathcote estuary

Cell		15	16	17	18	19	20	21	22	23	24	25	26
Chainage, km from Waimakariri River mouth		20.5 to 21	21 to 21.5	21.5 to 22.8	22.8 to 23.2	23.2 to 24.25	24.25 to 25.5	25.5 to 26.6	26.6 to 28.35	28.35 to 29	29 to 30	30 to 31.1	31.1 to 35.6
Morphology		Harbour beach	Harbour beach	Harbour beach	Harbour beach	Harbour beach	Harbour beach	Harbour beach	Harbour beach	Harbour beach	Harbour beach	Class 1 Structure	Class 1 Structure
Geology		Dune deposit	Dune deposit	Dune deposit	Dune deposit	Dune deposit	Dune deposit	Anthropic deposits	Anthropic deposits	Anthropic deposits	Estuarine deposit	Anthropic deposits	Anthropic deposits
Short-term (m)	Lower	-1	-1	-1	-1	-1	-1	-1	-1	-1	-1	N/A	N/A
	Mode	-3	-3	-3	-3	-3	-3	-3	-3	-3	-3		
	Upper	-5	-5	-5	-5	-5	-5	-5	-5	-5	-5		
Dune (m above toe)	Lower	1	0.8	1.1	1.2	0.6	0.8	1.5	1.5	1.8	0.8	1.8	3
	Mode	1.6	1	1.3	1.5	0.8	1	2	2.5	2	1	1.9	3.5
	Upper	2.3	1.5	1.8	2	1.5	2	3.5	3	2.5	1.5	2.0	4
Stable angle (deg)	Lower	30	30	30	30	30	30	30	30	30	30	18	18
	Mode	32	32	32	32	32	32	32	32	32	32	22	22
	Upper	34	34	34	34	34	34	34	34	34	34	26.6	26.6
Long-term (m) -ve erosion +ve accretion	Lower	0	0	-0.18	-0.18	-0.18	-0.18	-0.18	-0.18	-0.15	-0.15	N/A	N/A
	Mode	0.15	0.05	-0.15	-0.15	-0.15	-0.15	-0.15	-0.15	-0.13	-0.13		
	Upper	0.30	0.08	-0.12	-0.12	-0.07	-0.07	-0.05	-0.05	0	0		
Closure slope	Lower	0.05	0.05	0.05	0.05	0.05	0.05	0.08	0.08	0.08	0.05	N/A	N/A
	Mode	0.06	0.06	0.06	0.06	0.08	0.08	0.1	0.1	0.1	0.06		
	Upper	0.08	0.1	0.1	0.1	0.1	0.12	0.12	0.12	0.12	0.08		

4.5 Banks Peninsula harbours (detailed sites)

Banks Peninsula comprises two large Miocene composite volcanic cones where the central areas have collapsed and been eroded. Subsequent drowning by the sea has resulted in the formation of Lyttleton and Akaroa Harbours. The present-day harbour morphologies are the product of weathering and marine incision of the crater remnants over millions of years (Hart, 2009). The heads of both harbours are characterised by shallow intertidal flats which have gradually infilled with the predominantly fine-grained loess and volcanic sediment runoff from their surrounding catchments.

Lyttelton Harbour (Whakaraupō) is on the northern side of the Peninsula and is a 15 km long, rock-walled inlet with an average width of approximately 2 km. The steep rocky slopes descend to a near-flat seabed with a maximum depth of 15.5 m below MLWS. The upper harbour comprises three bay, Governor's Bay, Head of the Bay and Charteris Bay separated by peninsulas and Quail Island.

Lyttelton Harbour also includes the Port of Lyttelton which was constructed between 1863 and 1876. Large scale dredging has occurred since 1876 and historically dredged sediment was deposited at Camp Bay, Little Port Cooper and Gollans Bay. Since 1990 the dredged sediment has been deposited on the northern side of the harbour inlet (Livingston, Breeze and Mechanics Bay) (Hart, 2013).

Akaroa Harbour is on the southern side of Banks Peninsula and is approximately 17 km long with an average width of 2 to 3 km. The upper harbour is surrounded by a radial pattern of hills and valleys while the lower harbour shoreline is dominated by steep cliffs of basalt and andesite rock. Maximum water depths at the harbour entrance are 25 m and reduce to 10 m along the southern 9.5 km. The bays in the upper harbour (e.g. Duvauchelle and Takamatua) are predominantly sandy silt with very shallow intertidal flats and shore platforms. Bays in the middle section (e.g. Tikao and Akaroa) are mostly sand with some gravel and the southern bay (e.g. Wainui) comprises gravel.

Sites with detailed assessments include the harbour beach and bank shorelines where substantial development has occurred, including Corsair Bay, Cass Bay, Rapaki Bay, Charteris Bay, Hays Bay, Purau, Akaroa, Takamatua Bay, Duvauchelle Bay and Wainui (Figure 4.33 and Figure 4.34). As stated in Section 3.4.3, there is limited data available to assess these sites with a full probabilistic, detailed approach and therefore generic assumptions have been made around several of the parameter bounds, resulting in a quasi-probabilistic approach.

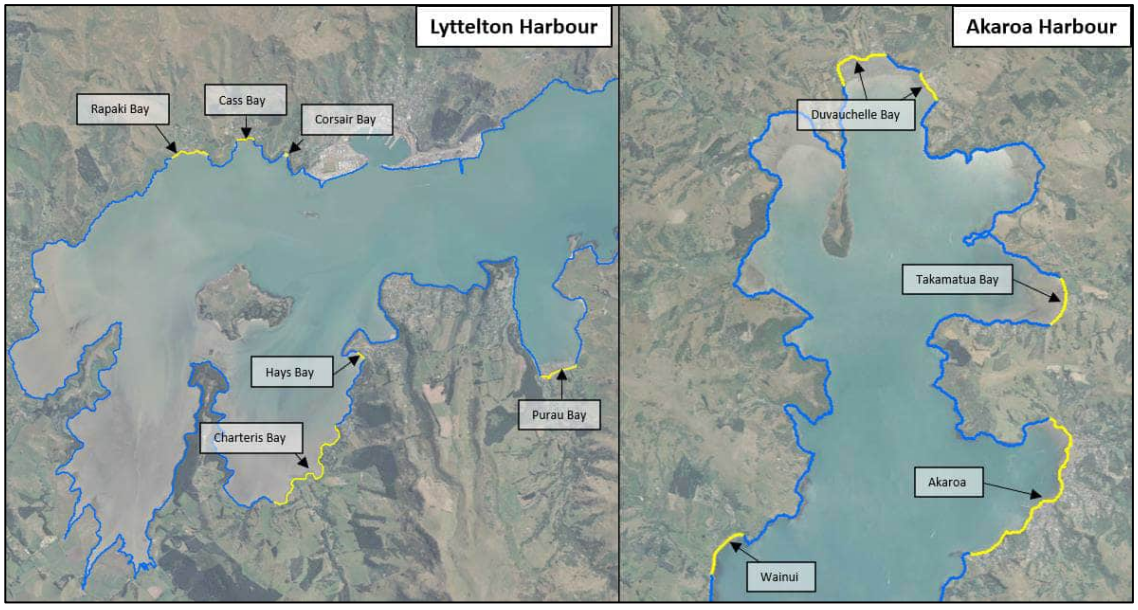

Figure 4.33: Overview map of detailed sites (yellow line) within the harbours.

Figure 4.34: Site photos (taken August 2020) along the Lyttelton and Akaroa harbour shorelines. (Top left) Cass Bay, (top right) Charteris Bay, (centre left) Purau Bay, (centre right) Akaroa (bottom left) Takamatua Bay, (bottom right) Wainui.

4.5.1 Short term component (ST)

The storm term component for the harbour beaches has been assessed using the same Kriebel & Dean (1993) method as adopted for the ST component within the Avon-Heathcote estuary (see Section 4.4.2). The storm tide levels and wave heights used to assess the short term component within Lyttelton and Akaroa Harbours are shown in Table 4.25 . Based on LiDAR, a range of different berm elevations with an upper slope of 5(H):1(V) has been assessed. Results indicate the short term component ranges from -2 to -8 m.

While there is some variation in the exposure of the harbour beaches, most of the sites are fronted with tidal flats which dissipate wave energy and therefore the depth-limited wave heights at each

site are similar. Subsequently, the short term parameter bounds for all harbour sites has been assumed the same. For the consolidated banks the short term component is not applicable as the banks behave differently to the unconsolidated beaches (see Section 3.1.3).

Table 4.25: Summary of storm tide and wave heights used to assess storm cut on the beaches within Lyttelton and Akaroa Harbours

	Lyttelton storm tide level (m NZVD)[1]	Akaroa storm tide level (m NZVD)[1]	Breaking wave height[2] (m)	Storm cut (m)
Lower bound	1.45	1.69	0.8	-2
Mode	1.67	1.90	1.2	-4
Upper bound	1.88	2.12	1.5	-6

[1] Based on 1 year, 10 year and 100 year storm tide levels.

[2] Based on SWAN model outputs for the average 1 year, 10 year and 100 year ARI wind speeds (see Appendix A).

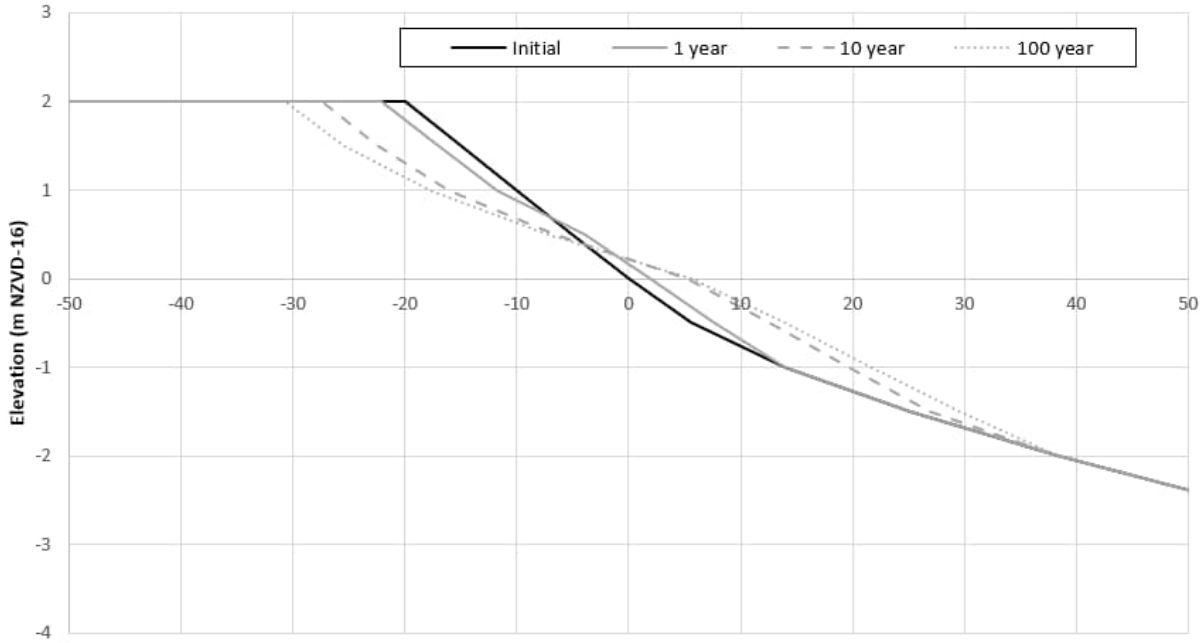

Figure 4.35: Example of beach response under different storm conditions within Lyttelton Harbour.

4.5.2 Long-term trends (LT)

Long-term trends within the harbour sites have been assessed based on analysis of historic aerial photographs. For most of the harbour sites the earliest historic aerial available is 1970. A significant portion of the beach and bank shoreline within Lyttelton and Akaroa Harbours has some form of protection structure along the toe and subsequently, there are limited areas available to measure natural long-term rates in absence of the structures. Due to this limitation, long-term rates have been assessed at discrete locations on unprotected shorelines Figure 4.36 provides an example of LT trends measured along transects at the unprotected shoreline within Charteris Bay and Allandale.

In areas where protection structures exist it is difficult to determine long-term rates, however, in absence of the structures, erosion is likely to occur and hence the structure exists. Site observations show evidence of scour and overtopping around structures which also implies that in absence of the structure, shoreline retreat is likely to occur (Figure 4.37). Similarly, some of the unprotected shorelines show minimal erosion in the historic aerials, however based on site observations there is

evidence of undercutting and erosion, for example at Takamatua (Figure 4.38). In contrast, there are some sites which appear stable from the site observations and as expected show minimal movement in the historic aerials, for example Purau Bay and Cass Bay (Figure 4.39).

Subsequently adopted LT rates have been based on a combination of site observations and historic shoreline analysis. The shoreline analysis shows the highest rate of erosion occurring along the harbour beach shoreline within Charteris Bay, where the average rate of regression is -0.17 m/year since 1970 (Figure 4.36). Majority of the other unprotected harbour shorelines show lower erosion rates around 0 to -0.07 m/year, for example at Allandale (Figure 4.36).

For the bays where there are protection structures or evidence of active erosion the adopted LT rate ranges from -0.01 to -0.07 m/yr. These rates are based on the LT erosion measured at unprotected harbour sites. For the shorelines that appear stable and show no measurable erosion, a lower bound of 0 m/year has been adopted. The more stable shorelines tend to be within Lyttelton Harbour, such as Purau Bay and Hays Bay, whereas the detailed Akaroa sites tend to show more evidence of erosion. Adopted long-term trends for each cell are shown in Table 4.26 and Table 4.27.

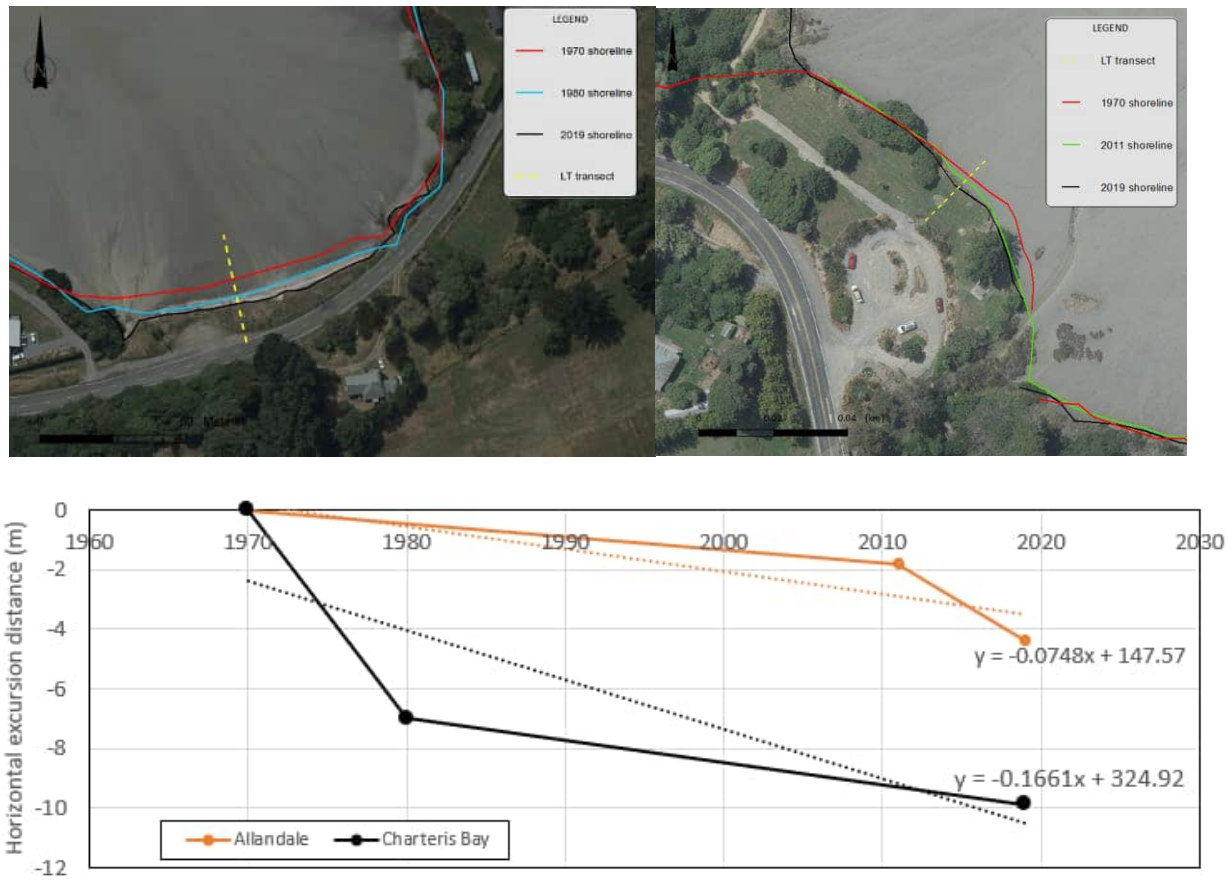

Figure 4.36: Example of shoreline analysis along transects at Charteris Bay (left) and Allandale (right).

Figure 4.37: Example of protection structures with evidence of scour and overtopping (Duvauchelle Bay).

Figure 4.38: Example of unprotected eroding harbour shorelines. (Left) Takamatua Bay, (right) Charteris Bay.

Figure 4.39: Example of stable unprotected harbour shorelines. (Left) Parau Bay, (right) Cass Bay.

4.5.3 Dune and bank stability (DS)

Dune and bank stability for the detailed sites around Lyttelton and Akaroa Harbours has been assessed as described in Section 4.1.3. Parameter bounds are defined based on the variation in dune/bank height within the coastal cell and potential range in stable angle of repose, which for beach sand is between 1(V):1.7(H) to 1(V):1.5(H) and for consolidated banks is assumed between 1(V):2(H) to 1(V):3(H). The slope stability for the underlying geology of the consolidated banks has not been included within this assessment, however based on the range of existing slopes, 1(V):2(H)

to 1(V):3(H) is appropriate. Adopted dune/bank heights and stable angles for each cell are shown in Table 4.26 and Table 4.27.

4.5.4 Response to sea level rise (SLR)

4.5.4.1 Harbour beaches

The beaches within Lyttelton and Akaroa Harbours consist of either silty sand, fine sand, shell or mixed sand and gravel and have a wide intertidal zone with no extensive dune system. Majority of the terrestrial sediments supplied to the beach areas are from the catchment via the streams that discharge to the coast and, to a lesser degree, from erosion from the cliff coasts adjacent. Therefore, they are expected to behave differently to sandy beaches in response to a rise in mean sea level. The same method as adopted for the SLR response within the Avon-Heathcote estuary has been adopted for the beaches within Lyttelton and Akaroa Harbours (see Section 4.4.5). Adopted slope values are summarised in Table 4.26 and Table 4.27.

4.5.4.2 Harbour banks

There are several detailed assessment sites within the harbours which include consolidated banks. These sites include Corsair Bay, Cass Bay, Rapaki Bay and part of Duvauchelle Bay. While shorelines like Corsair Bay and Cass Bay have sandy sediment along the foreshore, the backshore is characterised by consolidated material. These consolidated banks are likely to respond differently to SLR compared with the beaches.

Sea level rise may increase the amount of wave energy able to propagate over a fronting platform or beach to reach a bank/cliff toe, removing talus more effectively and increasing the potential for hydraulic processes to affect erosion and recession. However, in some locations, the existence of a talus will provide self-armouring, and may slow bank recession due to waves.

Aston et al. (2011) propose a generalised expression for future recession rates of cliff coastlines shown in Equation 4-6 where *LT* is the background erosion rate and S_1 is the historic rate of SLR, S_2 the rate of future SLR and *m* is the coefficient, determined by the response system (sea level rise response factor),

$$SL = LT\left(\frac{S_2}{S_1}\right)^m \quad (4\text{-}6)$$

An instantaneous response (m = 1) is where the rate of future recession is proportional to the increase in SLR. An instant response is typical of unconsolidated or weakly consolidated shorelines. No feedback (m = 0) indicates that wave influence is negligible and weathering dominates. The most likely response of consolidated shorelines is a negative/damped feedback system (m = 0.5), where rates of recession are slowed by development of a shore platform or fronting beach.

For the banks within the harbours a SLR response factor (m) ranging from 0.3 to 0.5 has been adopted. This is in line with what was used by T+T (2019) for the embankments within Tauranga Harbour which are likely to have similar erosion susceptibility as the harbour banks within Lyttelton and Akaroa Harbours

4.5.5 Summary of components

A summary of the adopted component values for detailed sites within Lyttleton Harbour and Akaroa Harbour is provided in Table 4.26 and Table 4.27.

4.5.6 Uncertainties

While some of the harbour sites have been completed at a detailed, quasi-probabilistic level, there is limited data availability and subsequently some key uncertainties exist:

- Long term erosion rates in absence of the protection structures, particularly within Corsair Bay, Charteris Bay, Duvauchelle and Wainui.
- Condition and design life of structures along the 'significantly modified shoreline' at Lyttelton Port and Akaroa township.
- Short term storm response. The Kriebel and Dean (1993) method does not account for different sediment types across the profile or response to short-duration events.
- Underlying geology and slope stability along the banks and hard cliffs.
- Shoreline response to SLR. Estuaries/harbours are areas of deposition and infilling so if sedimentation rates are high, the shoreline may adjust and keep pace, depending on the rate of SLR.

Table 4.26: Summary of adopted component values for the detailed sites within Lyttelton Harbour

Site		Lyttelton Port	Corsair Bay	Cass Bay	Cass Bay	Rapaki Bay	Rapaki Bay	Charteris Bay	Charteris Bay	Hays Bay	Purau
Cell		**31**	**32**	**33**	**34**	**35**	**36**	**42**	**43**	**44**	**45**
Chainage, km from Waimakariri River mouth		53.2 to 58.1 km	58.1 to 58.2 km	59 to 59.2 km	59.2 to 59.3 km	60.7 to 60.3 km	60.3 to 60.6 km	89.3 to 90.6 km	90.6 to 91.5 km	92.8 to 92.95 km	100.7 to 101.3 km
Morphology		Class 1 structure	Bank	Bank	Bank	Bank	Bank	Harbour beach	Bank	Harbour beach	Harbour beach
Geology		Anthropic deposits	Andesite	Andesite	Andesite	Loess	Loess	Estuarine deposit	Sandstone	Sand	Alluvial fan
Short-term (m)	Lower	N/A	N/A	N/A	N/A	N/A	N/A	-2	N/A	-2	-2
	Mode							-4		-4	-4
	Upper							-6		-6	-6
Dune (m above toe)	Lower	4.5	2	6	2	1.2	4	0.6	1.5	0.4	0.5
	Mode	5	2.5	9	3	1.5	5	0.8	2	0.5	1
	Upper	6	3.5	10	4	1.6	6	1	3	0.8	1.5
Stable angle (deg)	Lower	18	18	18	18	18	18	30	18	30	30
	Mode	22	22	22	22	22	22	32	22	32	32
	Upper	27	27	27	27	27	27	34	27	34	34
Long-term (m) -ve erosion +ve accretion	Lower	N/A	-0.07	-0.07	-0.07	-0.07	-0.07	-0.17	-0.07	-0.07	-0.07
	Mode		-0.02	-0.02	-0.02	-0.02	-0.02	-0.08	-0.02	-0.02	-0.02
	Upper		0	0	0	0	0	-0.05	0	0	0
Closure slope[1]/SLR factor[2]	Lower	N/A	0.3[2]	0.3[2]	0.3[2]	0.3[2]	0.3[2]	0.05[1]	0.3[2]	0.07[1]	0.06[1]
	Mode		0.4[2]	0.4[2]	0.4[2]	0.4[2]	0.4[2]	0.06[1]	0.4[2]	0.08[1]	0.08[1]
	Upper		0.5[2]	0.5[2]	0.5[2]	0.5[2]	0.5[2]	0.08[1]	0.5[2]	0.09[1]	0.09[1]

[1] Closure slope applicable for the harbour beach morphology

[2]SLR factor applicable for the bank morphology.

Table 4.27: Summary of adopted component values for the detailed sites within Akaroa Harbour

Site		Akaroa township	Akaroa township	Akaroa township	Akaroa township	Akaroa north	Childrens Bay	Takamatua Bay	Takamatua Bay	Duvauchelle	Duvauchelle	Duvauchelle	Wainui
Cell		69	70	71	72	73	74	75	76	79	80	81	91
Chainage, km from Waimakariri River mouth		310.1 to 311.5 km	311.5 to 312.1 km	312.1 to 312.8 km	312.8 to 313.6km	313.6 to 314 km	314 to 314.1km	319.3 to 320 km	320 to 320.9 km	328 to 328.5 km	328.5 to 329 km	329 to 330.1 km	344 to 344.9 km
Morphology		Class 1 structure	Class 1 structure	Class 1 structure	Class 1 structure	Bank	Bank	Bank	Beach	Beach	Bank	Beach	Beach
Geology		Alluvial fan	Alluvial fan	Alluvial fan	Alluvial fan	Loess	Loess	Loess	Beach deposit	Alluvial fan	Loess	Alluvial fan	Gravel
Short-term (m)	Lower	N/A	N/A	N/A	N/A	N/A	N/A	N/A	N/A	-2	N/A	-2	-2
	Mode									-4		-4	-4
	Upper									-6		-6	-6
Dune (m above toe)	Lower	2	2	1.5	1.5	5	0.4	2.5	1	0.7	2	0.3	2.7
	Mode	3	2.5	1.8	1.8	6	0.5	4	1.5	0.8	2.2	0.5	3.5
	Upper	5	3	2	2	8	1	6	2.5	1	2.5	1.5	4
Stable angle (deg)	Lower	18	18	18	18	18	30	18	18	30	18	30	30
	Mode	22	22	22	22	22	32	22	22	32	22	32	32
	Upper	26.6	26.6	26.6	26.6	26.6	34	26.6	26.6	34	27	34	34
Long-term (m) -ve erosion +ve accretion	Lower	N/A	N/A	N/A	N/A	-0.07	-0.07	-0.07	-0.07	-0.07	-0.07	-0.07	-0.07
	Mode					-0.02	-0.02	-0.02	-0.02	-0.02	-0.02	-0.02	-0.02
	Upper					-0.01	-0.01	-0.01	-0.01	-0.01	-0.01	-0.01	-0.01
Closure slope[1]/ SLR factor[2]	Lower	N/A	N/A	N/A	N/A	0.3[2]	0.06[1]	0.3[2]	0.3[2]	0.06[1]	0.3[2]	0.06[1]	0.08[1]
	Mode					0.4[2]	0.07[1]	0.4[2]	0.4[2]	0.07[1]	0.4[2]	0.07[1]	0.09[1]
	Upper					0.5[2]	0.08[1]	0.5[2]	0.5[2]	0.08[1]	0.5[2]	0.08[1]	0.10[1]

[1] Closure slope applicable for the Harbour beach morphology and SLR factor applicable for the bank morphology.

[2]SLR factor applicable for the bank morphology.

4.6 Banks Peninsula (regional sites)

Banks Peninsula is characterised by a radial pattern of drowned valleys and near-vertical plunging cliffs that terminate long sloping interfluves separating small bay-head beaches (Figure 4.40). The numerous bays of Banks Peninsula have formed as a result of flooding of the valleys by rising seas at the termination of the Pleistocene. Most of these embayments have filled with sediment composed of fine silts and clays, which were originally of aeolian or marine provenance. The beaches around Banks Peninsula vary from small pocket beaches with a mixture of sand gravel to more exposed fine sand beaches (Figure 4.41). Along many of the beaches the landward boundary is characterised by steep cliffs and banks (Dingwall, 1974). Figure 4.42 provides examples of the bank shorelines along undeveloped parts of Lyttelton and Akaroa harbours.

The Banks Peninsula sites have been completed at a regional hazard screening level with upper bound values adopted for each component.

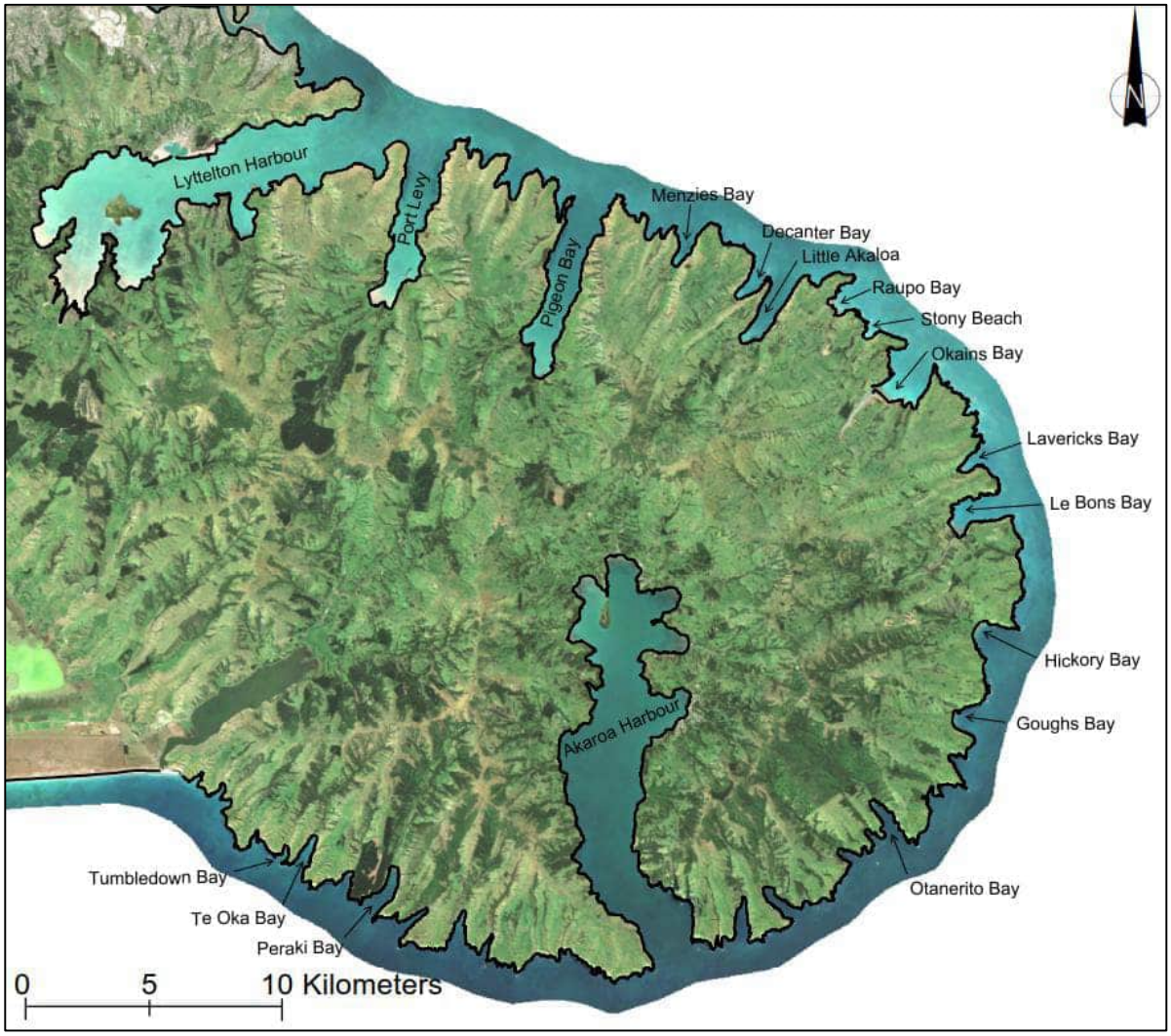

Figure 4.40: Overview of the bays and harbours around Banks Peninsula.

Figure 4.41: Examples of beach shorelines around Banks Peninsula. (Top left) Te Oka Bay, (top right) Okains Bay, (bottom left) Tumbledown Bay, (bottom right) French Farm Bay within Akaroa Harbour.

Figure 4.42: Examples of bank shorelines within the harbours around Banks Peninsula. (Left) Barry's Bay, Akaroa Harbour, (right) Ohinetahi, Lyttelton Harbour.

4.6.1 Short term component (ST)

There is limited data available to assess the short term storm cut along the Banks Peninsula beaches. Dingwall (1974) describes the bay-head beaches as generally stable or prograding, with the largest progradation in the north-eastern bays, such as Okains Bay. Beach surveying completed by Dingwall (1974) indicates storm cut up to 20 m at Le Bons and Hickory Bay.

For the regional screening assessment, generic storm cut distances have been adopted based on the beach exposure (i.e. a different distance will be adopted for sheltered and exposed beaches). The beaches have been broadly classified into 3 levels of exposure. Based on the level of exposure different short term values have been adopted as shown in Table 4.28. The storm cut on sheltered beaches is equivalent to the upper bound value for the detailed harbour beach sites. Sheltered beaches are those such as within the harbours and Port Levy. The storm cut for the exposed beaches is based on the findings from Dingwall (1974) and is approximately equivalent to the 100-year ARI storm cut on the Christchurch open coast. Exposed beaches are those such as Hickory and Le Bons Bay. Moderate exposure beaches include those within small bays such as Tumbledown Bay. It is

assumed that storm cut along the moderately exposed beaches is between the sheltered and exposed beach storm cut distances. Adopted short term values for each beach are provided in Table 4.29.

Table 4.28: Adopted short term values for different beach exposures around Banks Peninsula

Exposure	Adopted short term component (m)
Sheltered	-6
Moderate	-12
Exposed	-20

4.6.2 Dune and bank stability (DS)

Dune and bank stability has been assessed as described in Section 4.1.3. Dune and bank heights have been measured from the 2018 DEM. The upper bound heights measured within each cell have been adopted with an upper bound stable angle of repose. Adopted heights and stable slopes for each cell are shown in Table 4.29.

4.6.3 Long term component (LT)

The long term component has been assessed using end-point regression analysis from two shorelines (earliest and most recent shorelines available from aerial photographs). The maximum long term rate erosion rate identified within each coastal cell has been adopted.

The historic aerials show majority of the beaches are stable or accreting. Figure 4.43 shows an example of the long term accretion measured at Okains Bay. Dingwall (1974) also found the Banks Peninsula beaches to be either stable or accreting with the highest rate of sediment accumulation occurring within Okains Bay and a slightly lower rate at Le Bons bay. Multiple dune ridges within these bays also indicate periods of rapid coastal progradation.

The sediment is predominately derived from erosion and river supply along the South and mid Canterbury coast with northwards net sediment transport. The accretional trends are also consistent with the apparent accretion trends along south Pegasus Bay and Kaitorete Spit.

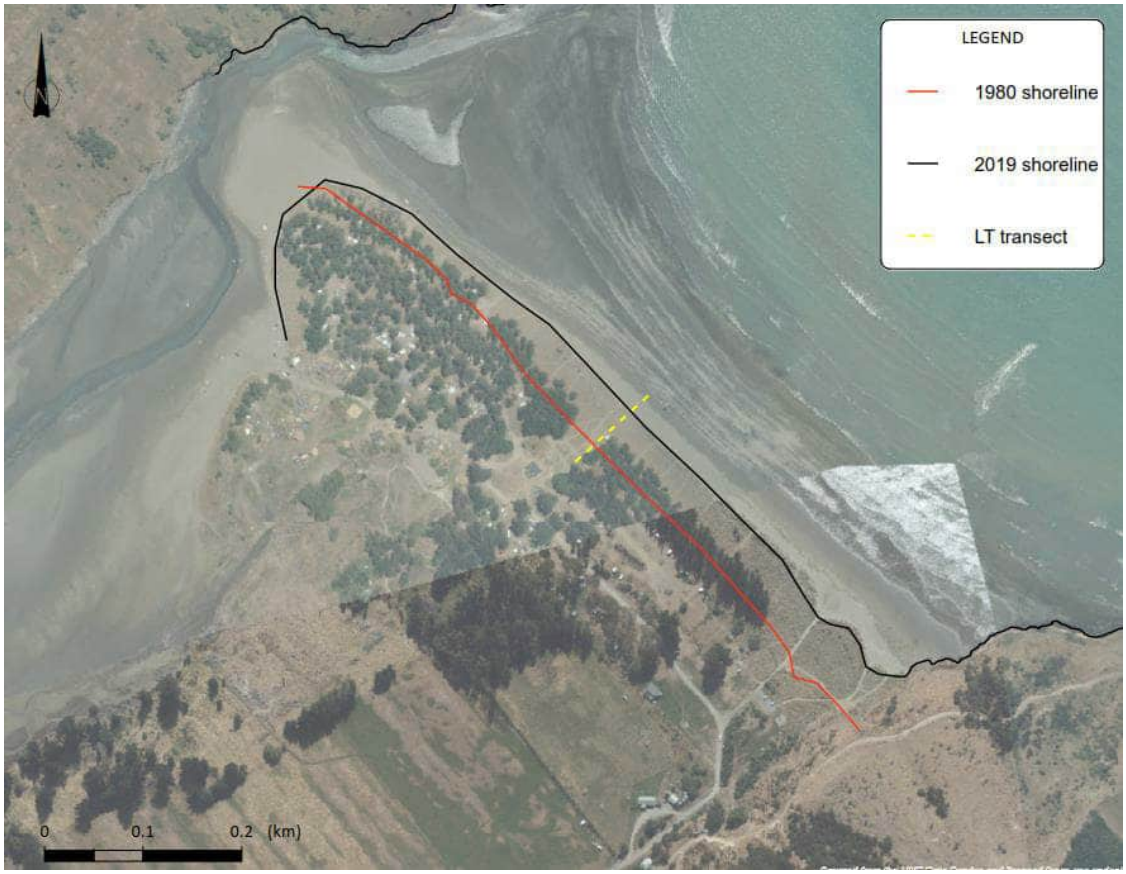

Figure 4.43: Example of shorelines used to assess long term trends in Okains Bay. Approximately 23 m of accretion measured between 1980 and 2019.

4.6.4 Response to SLR (SLR)

4.6.4.1 Beach response

For the sheltered beaches fronted by tidal flats, the SLR response has been assessed based on the modified Bruun Rule (see Section 4.4.5), using the upper beach slope. For the more exposed sandy beaches around Banks Peninsula, the standard Bruun model is more applicable with exchange occurring between the closure depth (see Section 0). However, due to limited wave statistics around the Peninsula it is difficult to define the closure depths for each beach. Subsequently, an assumed the closure slopes have been assumed the same as Taylors Mistake (0.02) which is a pocket beach with similar exposure as the Banks Peninsula beaches. Adopted slopes are included in Table 4.29.

4.6.4.2 Bank response

The bank response to SLR has been assessed based on the same response model outlined in Section 4.5.4.2 . An upper bound SLR response factor (*m*) of 0.5 has been adopted. This is in line with what was used by T+T (2019) for the embankments within Tauranga Harbour which are likely to have similar erosion susceptibility as the harbour banks around Lyttelton and Akaroa Harbours.

4.6.5 Cliff instability

Cliffs around Banks Peninsula are predominately basalt and andesite with greywacke-derived loess which forms an extensive mantle over the peninsula. The exposed cliffs around the edge of the Peninsula are near vertical with shore platforms in places (Figure 4.44). The cliffs within the bays tend to sit at lower angles and extend over 300 m high in places.

Figure 4.44: Example of cliff shorelines around Banks Peninsula.

The majority of the coastal cliffs around Banks Peninsula have existing slopes steeper than 1(H):1(V). The upper slopes which extend to over 500 m elevation tend to sit at a much lower angle, however the processes on these slopes are not substantially driven by coastal dynamics but instead are subject to more general slope instability hazard. This hazard is already identified and managed via the "Remainder of Port Hills and Banks Peninsula Slope Instability Management Area" in the Christchurch District Plan.

For coastlines where a "Cliff Collapse Management Area" or "Mass Movement Management Area" (either Class 1 or 2) is mapped in the Christchurch District Plan (e.g. Whitewash Head), this area has been used to define the width of the cliff instability component. The rationale for adopting this existing information rather than applying a separate regional screening analysis is that these management areas incorporate extensive site-specific geotechnical investigation, analysis of a range of trigger mechanisms and peer review which far exceeds the detail which is possible at a regional scale.

Where cliff collapse or mass movement management areas are not defined (i.e. remainder of Banks Peninsula), a simplified 3-step method based on the 2018 DEM has been used to define the width of the cliff instability component:

1 Where the slope is identified as being equal to or steeper than 1(H):1(V), the cliff slope has been identified as potentially unstable due to coastal processes (refer Figure 4.45).

2 A 20 m wide setback has been applied beyond the top of the steep cliff slope. This setback accounts for the physical scale of potential cliff failure mechanisms for typical cliff heights around Banks Peninsula. It also reflects the precision limitations involved in defining the top of the cliff at this regional scale. This 20 m setback value is at the upper end of the range of cliff retreat distances observed in the Canterbury Earthquakes, and of a similar scale to the width of the cliff collapse management areas defined in the district plan.

3 Where the coastal cliff edge is flatter than 1(H):1(V), a 30 m wide setback has been applied from the coastal edge. The 30 m setback is based on the average setback distance calculated for harbour beaches and banks for the 2130 1.5 m SLR scenario.

Historic aerial photographs indicate the long-term toe erosion of the Banks Peninsula cliffs is minimal and due to the scale and nature of the cliff assessment, it is not suitable to differentiate between current and future ASCE with different SLR scenarios therefore a single future ASCE is defined.

While this method is not a detailed cliff projection method, it is suitable for a regional coastal hazard screening assessment. It is emphasised that cliff collapse hazard is highly dependent on site-specific details and a can include a range of potential triggers in addition to coastal processes. These details

cannot be incorporated into this regional-scale assessment. If more detailed information is required about the cliff instability hazard for a specific location (e.g. as part of proposed development or hazard management activities in future) then a site-specific assessment should be undertaken, which may indicate that the hazard area is narrower or wider than mapped in this regional assessment.

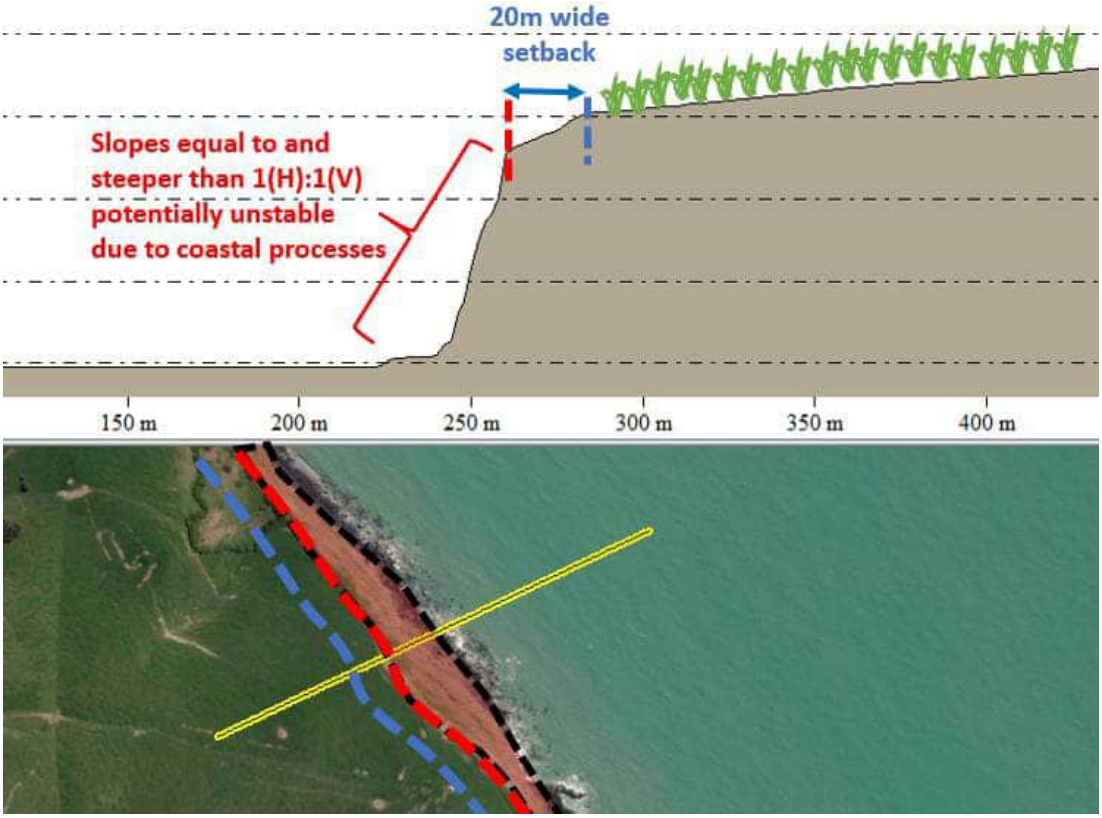

Figure 4.45: Example of cliff ASCE.

4.6.6 Summary of components

Adopted component values for the beaches and banks within regional hazard screening sites around Banks Peninsula are presented in Table 4.29.

4.6.7 Uncertainties

The regional hazard screening assessment includes a few uncertainties as outlined below:

- Long term erosion rates in absence of the protection structures.
- Short term storm response.
- Underlying geology and slope stability along the banks and hard cliffs.
- Shoreline response to SLR. Estuaries/harbours are areas of deposition and infilling so if sedimentation rates are high, the shoreline may adjust and keep pace, depending on the rate of SLR.
- Shoreline response to SLR on the outer Banks Peninsula beaches where there is limited data on offshore profiles and wave climate.

Table 4.29: Summary of adopted component values for the regional screening assessment beach and bank sites

Cell	Site	Chainage	Morph	Geology	Short-term (m)	Dune/bank height (m)	Stable Angle (deg)	Long-term (m/yr)	SLR component	
									Closure Slope	Factor
37	Sandy Beach Rd	64.7 to 67.1 km	Bank	Andesite	N/A	2	18	-0.07	N/A	0.5
38	Allandale	67.1 to 67.5 km	Beach	Alluvial fan	-6	1	30	-0.07	0.1	N/A
39	Teddington (low-lying)	73 to 81.3 km	Beach	Estuarine deposit	-6	0.8	30	-0.05	0.1	N/A
40	Moepuku (low-lying)	81.9 to 82.3 km	Bank	Loess	N/A	1.5	18	-0.05	N/A	0.5
41	Charteris Bay (west)	88.2 to 88.8 km	Bank	Sandstone	N/A	1.5	18	-0.07	N/A	0.5
46	Port Levy	122.1 to 123 km	Bank	Young alluvial fan	N/A	0.8	18	-0.07	N/A	0.5
47	Port Levy	123.5 to 123.7 km	Bank	Young alluvial fan	N/A	0.8	18	-0.07	N/A	0.5
48	Port Levy (Puari)	125 to 125.8 km	Beach	Young alluvial fan	-6	0.5	30	-0.05	0.1	N/A
49	Port Levy	126.1 to 126.8 km	Beach	Young alluvial fan	-6	1	30	-0.05	0.1	N/A
50	Holmes Bay	156.6 to 157.5 km	Beach	Young beach deposit	-6	1	30	-0.07	0.1	N/A
51	Pigeon Bay (south)	159.4 to 160.1 km	Beach	Young beach deposit	-6	2	30	-0.07	0.1	N/A
52	Pigeon Bay	160.4 to 161.2 km	Beach	Young alluvial fan	-6	2	30	-0.07	0.1	N/A
53	Menzies Bay	178 to 178.1 km	Beach	Young alluvial fan	-12	2	30	-0.07	0.1	N/A
54	Decanter Bay	186.5 to 186.7	Beach	Young alluvial fan	-12	1	30	-0.07	0.1	N/A
55	Little Akaloa	192.1 to 192.3 km	Beach	Young alluvial fan	-12	2.5	30	-0.07	0.1	N/A
56	Little Akaloa	192.3 to 192.5 km	Beach	Young alluvial fan	-12	3.5	30	-0.07	0.1	N/A
57	Raupo Bay	202 to 202.4 km	Beach	Young alluvial fan	-12	1	30	0	0.02	N/A
58	Raupo Bay	202.9 to 202.1 km	Beach	Young alluvial fan	-12	1	30	0	0.02	N/A
59	Stony beach	206.9 to 207.3 km	Beach	Young alluvial fan	-12	2.5	30	0	0.02	N/A
60	Okains Bay	213.3 to 214.3 km	Beach	Young beach deposit	-20	1	30	1	0.02	N/A
61	Lavericks	227.7 to 228.2 km	Beach	Young alluvial fan	-20	2	30	0	0.02	N/A
62	Le Bons Bay	235.6 to 236.1 km	Beach	Young beach deposit	-20	2	30	0.3	0.02	N/A
63	Le Bons Bay	236.1 to 236.5 km	Beach	Young beach deposit	-20	1	30	0.1	0.02	N/A

Table 4.29 (continued): Summary of adopted component values for the regional screening assessment beach and bank sites

Cell	Site	Chainage	Morph	Geology	Short-term (m)	Dune/bank height (m)	Stable Angle (deg)	Long-term (m/yr)	SLR component	
									Closure Slope	Factor
64	Hickory	247.8 to 248.5km	Beach	Young alluvial fan	-20	3	30	0	0.02	N/A
65	Goughs Bay	254 to 254.5 km	Beach	Young beach deposit	-20	2	30	0	0.02	N/A
66	Otanerito Bay	270.2 to 270.5 km	Beach	Young alluvial fan	-12	2	30	0	0.02	N/A
67	The Kaik	308.1 to 308.4 km	Bank	Loess	N/A	2	18	-0.07	N/A	0.5
68	Akaroa south	310.1 to 310.8 km	Bank	Loess	N/A	3	18	-0.07	N/A	0.5
77	Robinsons Bay south	324.3 to 324.6 km	Bank	Loess	N/A	4	18	-0.07	N/A	0.5
78	Robinsons Bay	324.6 to 325.6 km	Beach	Young alluvial fan	-6	1.5	30	-0.07	0.1	N/A
82	Barrys Bay (landfill)	332.1 to 332.4 km	Bank	Loess	N/A	4.5	18	-0.07	N/A	0.5
83	Barrys Bay	332.4 to 332.7 km	Bank	Loess	N/A	1.5	18	-0.07	N/A	0.5
84	Barrys Bay	332.7 to 333 km	Bank	Loess	N/A	2.5	18	-0.07	N/A	0.5
85	Barrys Bay	333 to 333.6 km	Beach	Young alluvial fan	-6	0.9	30	-0.05	0.1	N/A
86	Barrys Bay (south)	333.6 to 334.6 km	Bank	Loess	N/A	4	18	-0.07	N/A	0.5
87	French farm bay (boat houses)	335.5 to 335.8 km	Bank	Loess	N/A	2	18	-0.07	N/A	0.5
88	French farm bay	335.8 to 336.5 km	Beach	Young alluvial fan	-6	1.5	30	-0.05	0.1	N/A
89	Tikao Bay	340.9 to 341.1 km	Bank	Basalt	N/A	2	18	-0.07	N/A	0.5
90	Tikao Bay	341.4 to 341.8 km	Bank	Loess	N/A	3.5	18	-0.07	N/A	0.5
92	Wainui south	344.9 to 346.2 km	Bank	Loess	N/A	4	18	-0.07	N/A	0.5
93	Peraki Bay	390.2 to 390.6 km	Beach	Young alluvial fan	-12	2	30	0	0.02	N/A
94	Te Oka Bay	401.3 to 401.5 km	Beach	Young alluvial fan	-12	3	30	0	0.02	N/A
95	Tumbledown Bay	404.6 to 405 km	Beach	Young alluvial fan	-12	3	30	0	0.02	N/A

4.7 Kaitorete Spit

The Kaitorete Spit is located on the southern side of Banks Peninsula on the Canterbury Bight. The spit extends for approximately 26 km and is over 2 km wide at its widest extent. The sediment forming the spit is predominately gravel (Figure 4.46).

The barrier spit is understood to have existed for the last 8,000 years. The barrier initially developed as a spit extending north from near the Rakaia River mouth, during the sea level rise in the Late Pleistocene and Early Holocene. During the mid-Holocene the spit extended to Banks Peninsula creating a barrier lake complex behind the spit. Since the end of the Holocene transgression the whole coastline has been relatively stable (Soons et al., 1997).

Figure 4.46: Site photos (taken August 2020) near Birdlings Flat at the northern extent of Kaitorete Spit.

4.7.1 Cell splits

The Kaitorete Spit has been split into 5 cells (Figure 4.47). The cell split is largely based on the variation in long term trends along the shoreline.

Figure 4.47: Overview of cell splits and profile locations along Kaitorete Spit.

4.7.2 Short term component (ST)

The short term component along Kaitorete Spit has been assessed using the beach profile dataset. Figure 4.48 provides an example of the beach profiles measured at ECE3755 near Birdlings Flat. Based on visual inspection the berm toe along Kaitorete Spit is estimated to be around 6 m RL.

The short-term component has been quantified using statistical analysis of the inter-survey storm cut distances. The inter-survey storm cut distance is the landward horizontal retreat distance measured between two consecutive surveys (Figure 4.48).

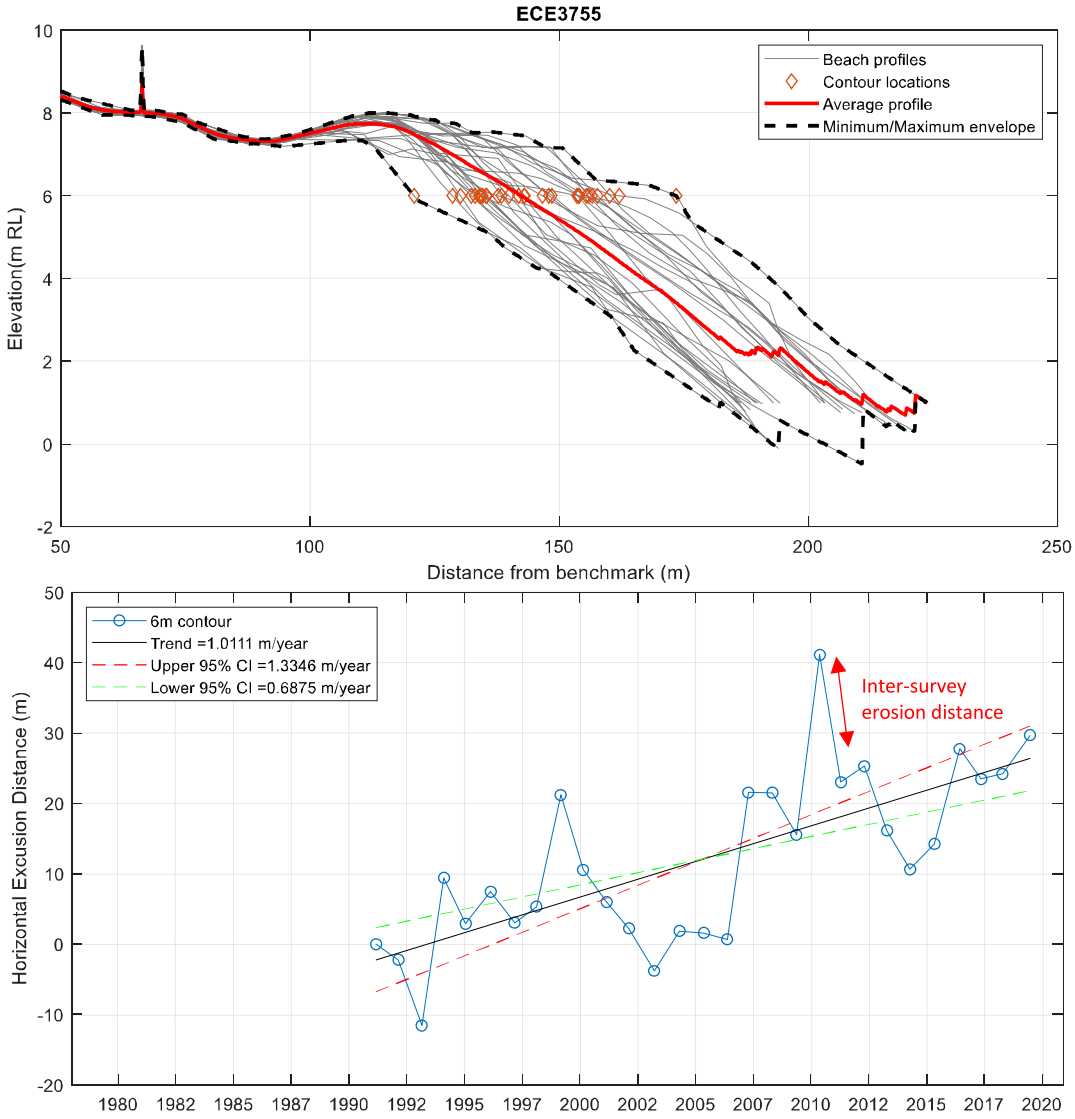

Figure 4.48: Example of beach profile ECE3755 used to assess short term erosion along the Kaitorete Spit.

Based on Extreme Value Analysis (EVA), using the inter-survey erosion distances for each beach profile, the 100 year ARI inter-survey storm cut distance ranges from 5 to 20 m. An example of the extreme value curve for profile ECE3800 is shown in Figure 4.49. For this assessment 20 m storm cut has been adopted for all cells along the spit.

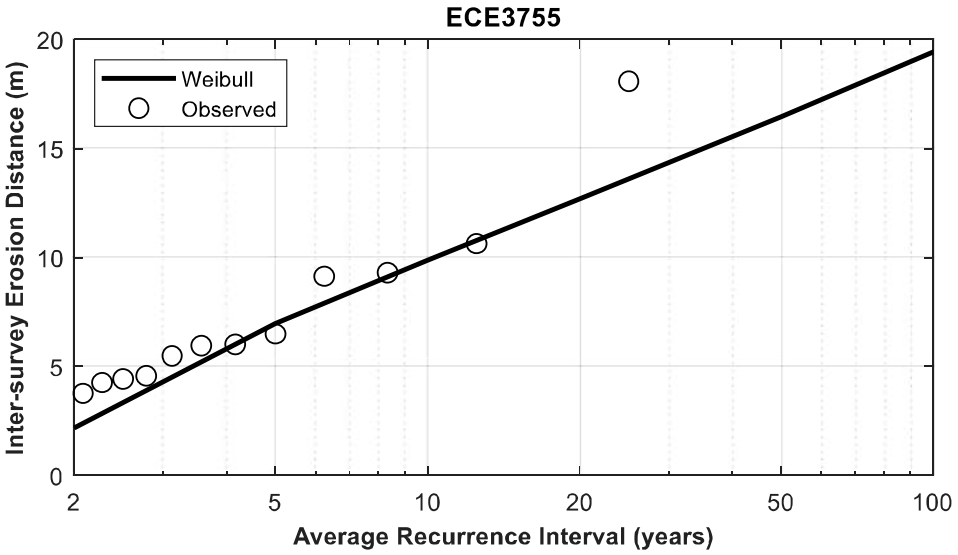

Figure 4.49: Example of extreme value curve for inter-survey storm cut distances at profile ECE3755 on Kaitorete Spit.

4.7.3 Long-term trends (LT)

Long-term shoreline changes have been assessed using a combination of beach profiles and historic shorelines. Linear regression analysis has been completed for both datasets and comparisons made to infer the long-term rates within each coastal cell.

The beach profiles include data from 1991 to 2019 and show a trend of erosion at the southern end of the spit and accretion at the northern end. Figure 4.50 shows erosion up to -0.6 m/year at the southern end and accretion over 1 m/year at the northern end. These profile trends are consistent with both the historic shorelines (Figure 4.51) and the findings from Measures et al (2014) and Cope (2018).

The shoreline retreat appears to greatest at ECE1620 (approximately 6 km north of Taumutu). North of ECE1620, the rates of retreat reduce until there is a complete switch to shoreline accretion around profile ECE2995. The accretion increases along the northern 10 km of the spit towards Birdlings Flat. Cope (2018) describes this transition between shoreline erosion and shoreline progradation as a hinge point where clockwise shoreline rotation is continuing to occur. The spit has formed through longshore drift northwards from the Rakaia River. The shoreline at Rakaia mouth has eroded and slowly changed shoreline angle which has reduced the sediment transport and resulted in the hinge point migrating north (Measures et al., 2014).

The maximum long term rate erosion rate identified within each coastal cell has been adopted and is shown in Table 4.30.

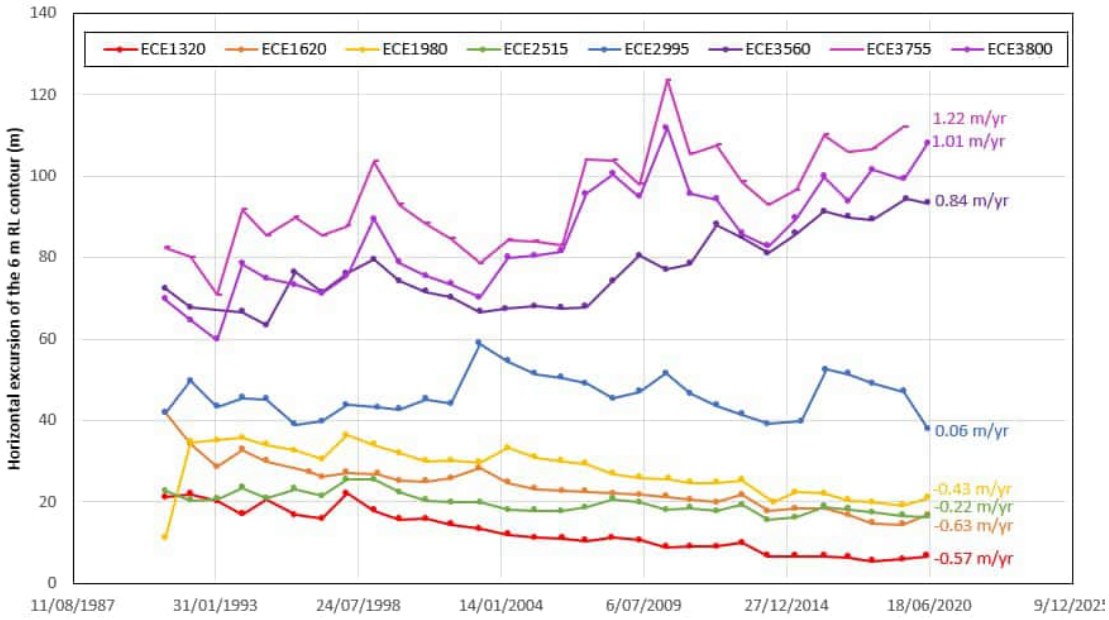

Figure 4.50: Horizontal excursion distances measured at the berm toe for profiles along Kaitorete Spit.

Figure 4.51: Historic shorelines along the northern end of Kaitorete Spit showing up to 80 m accretion since 1980.

4.7.4 Response to sea level rise (SLR)

Shoreline response to SLR along Kaitorete Spit has been assessed using a modification of the Bruun rule (Equation 4.7 and Figure 4.52). Instead of adopting closure depths based on offshore wave heights, the closure depth along mixed sand gravel beaches has been assumed to be equivalent to the beach step.

The beach step marks the lower extent of the active beach. Typically, on sand gravel beaches the gravel portion of the shoreface rarely extends below the low tide mark (Shulmeister and Jennings, 2009). As there is limited offshore survey data to determine the location of the beach step along Kaitorete Spit, the beach step has been assumed 5 m below MSL and approximately 60 m offshore from the MSL contour. This is consistent with the estimate made by Measures et al (2014) (i.e. -5.5 m LVD37 at Taumutu).

$$Retreat\ due\ to\ SLR = SLR\frac{L}{h} \quad (4.7)$$

Where:

SLR = SLR (m).

L = Horizontal distance from beach step to the berm crest.

h = height of the berm above the beach step.

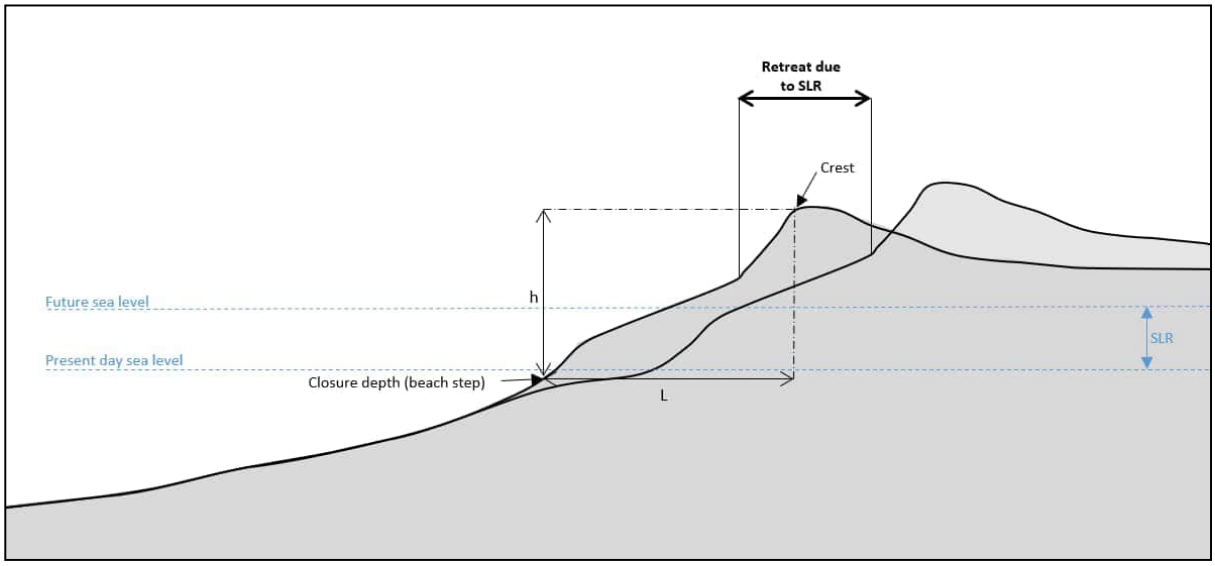

Figure 4.52: Conceptual diagram of SLR response along mixed sand gravel beach.

4.7.5 Summary of components

Adopted component values for the Kaitorete Spit are shown in Table 4.30.

4.7.6 Uncertainties

Key uncertainties in the erosion hazard assessment for Kaitorete Spit include:

- Future sediment supply from the Rakaia River.
- Offshore profile and subsequently the shoreline response to SLR.

Table 4.30: Summary of adopted components along the Kaitorete Spit

Cell	Name	Chainage (km)	Morphology	Geology	Short-term (m)	Berm height (m above toe, 6 m RL)	Stable Angle (deg)	Long-term (m/yr)	SLR response slope
96	Birdlings Flat	419 to 424.5	Gravel beach	Gravel	-20	2.5	30	0.8	0.07
97	Kaitorete Spit	424.5 to 432	Gravel beach	Gravel	-20	2.5	30	0.06	0.07
98	Kaitorete Spit	432 to 438.5	Gravel beach	Gravel	-20	6	30	-0.4	0.07
99	Kaitorete Spit	438.5 to 442	Gravel beach	Gravel	-20	6	30	-0.6	0.07
100	Kaitorete Spit	442 to 446	Gravel beach	Gravel	-20	0.5	30	-0.6	0.07

5 Coastal erosion results

For each coastal cell, the relevant components influencing the ASCE have been combined as described in Section 3.1.1. The following section provides an overview of the results for each area. Erosion distances are summarised within the following tables, which for detailed sites, include the P66% and P5% ASCE and for the regional screening sites, include the single ASCE distance for each scenario. The P66% represents the distance at which there is 66% probability of the shoreline eroding beyond and can be considered a likely scenario. The P5% represents the distance at which there is 5% probability of the shoreline eroding beyond and can be considered as the extent to which it is possible but very unlikely for the shoreline to retreat to (P5% is taken as the middle of the IPCC (2013) "very unlikely" range of 0 - 10% probability). The P5% ASCE from the detailed scale assessments and the ASCE from the regional scale assessments are approximately equivalent, representing the 'upper end' erosion distances.

Coastal erosion maps, including the full probabilistic results for each of the detailed sites is available on the website viewer (refer Section 1.3). Overview maps which show the variation in erosion distances across the district are provided in Appendix E.

5.1 Christchurch open coast

The P66% and P5% ASCE distances along the Christchurch open coast are presented in Table 5.1. The current ASCE is dominated by the short-term storm erosion and tends to be largest towards the north where storm cut was found to be slightly larger. The short-term storm response also dominates the future ASCE under the shorter timeframes (i.e. 2050), accounting for over 50% of the total ASCE distance in most cells.

Seawalls are present within Cells 7 and 9, however these structures have not been accounted for within the assessment. The ASCE within these cells represents the hazard in absence of the structures, and therefore, while these structures remain functional, the ASCE is likely to be an overprediction.

The long-term trends are a key factor influencing the variation in the future ASCE along the Christchurch open coast. Most of the shoreline has historically shown long-term accretion trends due to the sediment supply from the Waimakariri River. The accretion rates tend to increase southwards and are largest within Cell 13, where the future ASCE are seaward of the current shoreline position. The high accretion rates at the southern end of the shoreline are likely a result of the net southward sediment transport and interactions with the ebb tidal delta. Over time the shoreline may slightly adjust orientation, with erosion towards the north and accretion towards the south, until an equilibrium is reached.

Due to the high accretion rates at the southern end of the shoreline (i.e. Cells 9 to 14), the future ASCE within these cells is most sensitive to changes in sediment supply from the Waimakariri River. A 28% increase in sediment supply from the Waimakariri River could reduce the 2130 1.5 m SLR ASCE by up to 27 m within Cell 13, and a 11% decrease in sediment supply could increase the future ASCE distance by 14 m. As long-term trends are smaller at the northern end of the beach (i.e. Cells 2 to 8), the future ASCE is less sensitive to changes in sediment supply. For example, within Cell 6, a 28% increase or an 11% decrease in sediment supply would result in the future 2130 1.5 m SLR ASCE shifting either seaward 5 m or landward 2 m.

The future ASCE are also influenced by the amount of SLR. Under low SLR scenarios the impact from long term accretion is likely to counteract any potential recession due to SLR, however higher SLR (e.g. more than about 0.4 – 0.6 m by 2130) is expected to overtake the impact of accretion and result in shoreline retreat. The tipping point at which SLR overtakes any impact of long-term accretion is dependent on the SLR scenario. For example, by 2080 under low SLR (i.e. 0.4 m), the

long-term accretion within Cell 13 dominates, whereas under a high SLR (i.e. 1.5 m) scenario there is a tipping point where erosion due to SLR dominates.

There is high uncertainty around the future erosion rates at the distal end of the Southshore Spit. As mentioned in Section 4.1.4, an increased tidal prism within the estuary is likely to enlarge in the tidal inlet and potentially increase erosion on the spit. However, quantification of this would require detailed investigation and modelling which is beyond the scope of this assessment. The previous assessment (T+T, 2017) adopted the most landward shoreline extent over the last 80 years, which provides more conservatism but still does not account for uncertainty of future processes.

Table 5.1: ASCE widths (m) for the P66% ('likely') and P5% ('very unlikely') ASCE along Christchurch Open Coast

Cell	Probability												28% increase in sediment supply	11% decrease in sediment supply
		Current	2050		2080			2130					2130	2130
		0 m SLR	0.2 m SLR	0.4 m SLR	0.4 m SLR	0.6 m SLR	0.8 m SLR	0.4 m SLR	0.6 m SLR	0.8 m SLR	1 m SLR	1.2 m SLR	1.5 m SLR	1.5m SLR	1.5m SLR
	P66%	-10	-14	-20	-15	-21	-27	-7	-13	-20	-26	-32	-41	-17	-54
1	P5%	-24	-36	-43	-53	-61	-68	-71	-78	-85	-93	-101	-112	-89	-126
	P66%	-10	-9	-15	-8	-14	-19	5	-1	-7	-13	-18	-27	-16	-32
2	P5%	-23	-23	-30	-23	-31	-40	-11	-19	-28	-37	-46	-60	-51	-66
	P66%	-9	-8	-14	-7	-13	-19	6	-1	-7	-13	-19	-29	-18	-34
3	P5%	-22	-21	-28	-21	-27	-34	-9	-15	-22	-29	-36	-46	-37	-52
	P66%	-9	-10	-17	-12	-18	-24	-4	-10	-16	-22	-28	-37	-30	-41
4	P5%	-22	-23	-30	-26	-33	-41	-18	-25	-33	-41	-49	-61	-54	-64
	P66%	-8	-12	-18	-16	-22	-28	-13	-19	-25	-31	-37	-46	-42	-48
5	P5%	-15	-20	-27	-25	-33	-41	-23	-31	-39	-47	-55	-67	-64	-70
	P66%	-8	-14	-22	-19	-28	-36	-14	-23	-31	-39	-48	-60	-55	-63
6	P5%	-15	-22	-31	-30	-40	-50	-29	-39	-49	-59	-69	-85	-82	-87
	P66%	-4	-10	-19	-16	-24	-32	-11	-19	-28	-36	-44	-57	-52	-59
7	P5%	-11	-18	-28	-27	-36	-47	-25	-35	-45	-55	-66	-81	-79	-84
	P66%	-7	-11	-17	-15	-20	-26	-10	-16	-22	-27	-33	-41	-37	-44
8	P5%	-14	-20	-29	-27	-37	-47	-26	-35	-45	-54	-64	-80	-76	-81
	P66%	-5	-5	-11	-4	-10	-17	9	2	-4	-11	-17	-27	-17	-32
9	P5%	-12	-14	-26	-19	-31	-43	-10	-21	-33	-46	-58	-77	-68	-82
	P66%	-7	-8	-14	-8	-13	-19	2	-3	-9	-14	-20	-28	-20	-33
10	P5%	-14	-18	-29	-24	-36	-48	-15	-27	-39	-51	-63	-82	-74	-86
	P66%	-6	-6	-14	-4	-12	-19	11	3	-5	-12	-19	-30	-18	-37
11	P5%	-13	-15	-28	-20	-33	-47	-7	-20	-33	-47	-60	-81	-70	-87

Table 5.1 (continued): ASCE widths (m) for the P66% ('likely') and P5% ('very unlikely') ASCE along Christchurch Open Coast

Cell	Probability												28% increase in sediment supply	11% decrease in sediment supply
		Current	2050		2080			2130					2130	2130
		0 m SLR	0.2 m SLR	0.4 m SLR	0.4 m SLR	0.6 m SLR	0.8 m SLR	0.4 m SLR	0.6 m SLR	0.8 m SLR	1 m SLR	1.2 m SLR	1.5 m SLR	1.5m SLR	1.5m SLR
	P66%	-6	-2	-9	4	-3	-11	26	18	11	3	-4	-15	3	-24
12	P5%	-13	-11	-24	-11	-24	-38	+11	-3	-16	-30	-44	-65	-47	-75
	P66%	-5	6	-1	18	11	4	51	43	36	29	22	11	38	-3
13	P5%	-12	-3	-14	+5	-7	-19	+37	+25	+13	0	-12	-31	-4	-45
	P66%	-8	-7	-15	-6	-14	-22	11	3	-5	-13	-21	-33	-19	-41
14	P5%	-13	-19	-30	-28	-39	-50	-25	-36	-46	-57	-69	-86	-78	-91

*Negative values are erosion and positive values are accretion.

5.2 Sumner

The ASCE distances for the P66% and P5% along Sumner are presented in Table 5.2. Cells 27 and 29 are classified as Class 1 structures (see Section 3.1.5). The ASCE within these two cells represents the immediate hazard is the structures were to fail and is a function of the structure height and stable angle of repose for the filled material. The future ASCE has been set equivalent to the current ASCE, which would be the case if the structures were promptly repaired if damaged. However, if the protection structures fail and are not promptly repaired then it is likely the shoreline will rapidly erode.

The current ASCE within Cell 28 represents the potential short-term storm cut and dune instability and is relatively small due to the significant volume of sand on the beach providing protection to the dunes along Clifton Beach. The future P5% ASCE ranges from -8 m by 2050 under low SLR, to -73 m by 2130 under high SLR. While there has been long-term accretion within Cell 28, the impacts of SLR are likely to overtake any long-term accretion.

There is high uncertainty around the future accretion rates within Cell 28. As mentioned in Section 4.2.4, an increased tidal prism within the estuary is likely to result in an enlarged tidal inlet and potentially increased erosion along the Clifton Beach shoreline.

Table 5.2: ASCE widths (m) for the P66% ('likely') and P5% ('very unlikely') ASCE along Sumner

Cell	Probability of exceedance	Current	2050		2080			2130					
		0 m SLR	0.2 m SLR	0.4 m SLR	0.4 m SLR	0.6 m SLR	0.8 m SLR	0.4 m SLR	0.6 m SLR	0.8 m SLR	1 m SLR	1.2 m SLR	1.5 m SLR
27	P66%	-6	-6	-6	-6	-6	-6	-6	-6	-6	-6	-6	-6
	P5%	-8	-8	-8	-8	-8	-8	-8	-8	-8	-8	-8	-8
28	P66%	-1	-2	-9	-2	-9	-16	10	3	-5	-12	-19	-30
	P5%	-3	-8	-21	-15	-27	-40	-7	-18	-30	-42	-54	-73
29	P66%	-4	-4	-4	-4	-4	-4	-4	-4	-4	-4	-4	-4
	P5%	-7	-7	-7	-7	-7	-7	-7	-7	-7	-7	-7	-7

5.3 Taylors Mistake

The ASCE distances for the P66% and P5% along Taylors Mistake are presented in Table 5.3. The current ASCE, which represents the potential short-term storm cut and dune instability, ranges from -7 to -13 m for the P66% to P5%.

By 2050 under low SLR, the future ASCE ranges from -13 to -22 m for the P66% to P5% and by 2130 under high SLR, the future ASCE ranges from -47 m to -96 m.

Over the shorter timeframes (i.e. by 2050), the erosion distance is dominated by the potential short-term storm response, which in 2050, contributes approximately 40 to 50% of the total erosion distance. Over longer timeframes (i.e. by 2130), the short-term erosion component contributes only 15 to 35% of the total erosion distance. Over time the impact of long-term trends and SLR increases and subsequently has a greater influence on the total erosion distance.

Table 5.3: ASCE widths (m) for the P66% ('likely') and P5% ('very unlikely') ASCE along Taylors Mistake

Cell	Probability of exceedance	Current	2050		2080			2130					
		0 m SLR	0.2 m SLR	0.4 m SLR	0.4 m SLR	0.6 m SLR	0.8 m SLR	0.4 m SLR	0.6 m SLR	0.8 m SLR	1 m SLR	1.2 m SLR	1.5 m SLR
30	P66%	-7	-13	-19	-19	-24	-30	-19	-24	-30	-35	-40	-47
	P5%	-13	-22	-32	-35	-45	-55	-40	-50	-60	-70	-80	-96

5.4 Avon-Heathcote Estuary

The ASCE distances for the P66% and P5% around the Avon-Heathcote estuary are presented in Table 5.4. The current ASCE represents the potential short-term storm cut and shoreline instability, which is relatively consistent across the estuary, ranging from -5 to -6 m for most cells.

Erosion protection structures, in varying condition, exist around the estuary and in these locations the current ASCE represents the immediate hazard if the structures were to fail. For Cell 15 to 24, the future ASCE has been assessed to represent the erosion hazard in absence of the structures.

Over shorter timeframes (i.e. by 2050) the ASCE distance is dominated by the potential short-term storm erosion which contributes 30 to 70% of the total erosion distance. Over longer timeframes (i.e. by 2080 and 2130), the long-term trends and response to SLR dominate the total erosion distance. Long-term erosion is largest within Cells 17 to 22, resulting in larger future ASCE, ranging from -35 to -48 m by 2130 under a high SLR scenario.

Cells 25 and 26 are classified as Class 1 structures (see Section 3.1.5). The ASCE within these two cells represents the immediate hazard if the structures were to fail and is a function of the structure height and stable angle of repose for the filled material. The ASCE is largest in Cell 26 where the structures are higher. The future ASCE have been set equivalent to the current ASCE, which would be the case if the structure was promptly repaired if damaged. However, if the protection structure fails and is not promptly repaired then it is likely the fill material will rapidly erode, and the shoreline will eventually move back towards its 'original' natural position (this scenario has not been modelled in this study).

Table 5.4: ASCE widths (m) for the P66% and P5% ASCE around the Avon-Heathcote Estuary

Cell	Probability of exceedance	Current	2050		2080			2130					
		0 m SLR	0.2 m SLR	0.4 m SLR	0.4 m SLR	0.6 m SLR	0.8 m SLR	0.4 m SLR	0.6 m SLR	0.8 m SLR	1 m SLR	1.2 m SLR	1.5 m SLR
	P66%	-4	-1	-5	2	-2	-5	12	8	5	2	-1	-5
15	P5%	-6	-6	-10	-8	-11	-14	-5	-8	-11	-15	-18	-22
	P66%	-4	-5	-8	-6	-9	-12	-4	-7	-10	-12	-13	-13
16	P5%	-5	-7	-11	-10	-13	-17	-9	-12	-15	-19	-21	-22
	P66%	-4	-11	-14	-18	-21	-24	-26	-29	-31	-34	-37	-39
17	P5%	-6	-13	-17	-21	-25	-28	-29	-33	-36	-40	-43	-47
	P66%	-4	-11	-14	-19	-21	-24	-26	-29	-31	-34	-37	-40
18	P5%	-6	-13	-17	-21	-25	-28	-30	-33	-36	-40	-43	-48
	P66%	-3	-10	-12	-16	-18	-19	-22	-24	-26	-27	-27	-27
19	P5%	-5	-12	-15	-19	-22	-25	-27	-30	-33	-35	-36	-37
	P66%	-4	-10	-12	-16	-18	-20	-22	-24	-26	-28	-30	-30
20	P5%	-5	-12	-15	-20	-23	-26	-28	-30	-33	-36	-38	-41
	P66%	-4	-10	-12	-15	-17	-19	-21	-23	-25	-27	-29	-31
21	P5%	-6	-13	-14	-19	-21	-23	-27	-29	-31	-33	-35	-38
	P66%	-4	-10	-12	-15	-17	-19	-21	-23	-25	-27	-29	-31
22	P5%	-6	-12	-14	-19	-21	-23	-27	-29	-31	-33	-35	-38
	P66%	-4	-9	-11	-13	-15	-17	-17	-19	-21	-23	-25	-27
23	P5%	-6	-11	-13	-17	-19	-21	-24	-26	-28	-30	-32	-35
	P66%	-4	-9	-13	-15	-18	-21	-19	-22	-26	-28	-30	-30
24	P5%	-5	-12	-15	-19	-23	-26	-26	-29	-33	-36	-38	-39
	P66%	-4	-4	-4	-4	-4	-4	-4	-4	-4	-4	-4	-4
25	P5%	-5	-5	-5	-5	-5	-5	-5	-5	-5	-5	-5	-5
	P66%	-8	-8	-8	-8	-8	-8	-8	-8	-8	-8	-8	-8
26	P5%	-10	-10	-10	-10	-10	-10	-10	-10	-10	-10	-10	-10

5.5 Harbours (detailed sites)

5.5.1 Lyttelton Harbour

The ASCE distances for the P66% and P5% around the detailed sites within Lyttelton Harbour are presented in Table 5.5. The current P5% ASCE is largest within Cass Bay (Cell 33) and Rapaki Bay (Cell 36), where the current ASCE accounts for potential instability of the high banks, ranging from -15 to -25 m. The current P5% ASCE along the harbour beaches (Charteris Bay, Hays Bay and Purau) is smaller, ranging from -6 to -7 m.

Erosion protection structures, in varying condition, exist around the Lyttelton Harbour sites and in these locations the current ASCE represents the immediate hazard if the structures were to fail. However, for the future ASCE, the structures have not been accounted for and the ASCE represents the erosion hazard in absence of the structures.

Long-term trends and SLR response are estimated to be relatively similar across the harbour sites. For the harbour beaches, the 2050 P5% ASCE under low SLR ranges from -10 to -12 m and by 2130

under high SLR is up to -32 m. For the harbour banks, the 2050 P5% ASCE under low SLR ranges from -6 to -27 m and by 2130 under high SLR, is up to -36 m.

For majority of the cells the short-term erosion (i.e. storm cut on beaches or bank instability) contributes to over 50% of the total erosion distance in 2050. Over time the impact of long-term trends and SLR response increases and subsequently has a greater influence on the total erosion distance.

Long-term erosion rates are assumed to be relatively similar across the harbour and therefore with no/low SLR there is little variation in the future ASCE. As with the current ASCE, the variation across the harbour banks is a function of the bank height, with higher banks having a larger ASCE. The harbour beaches, in particular Purau Bay, are more sensitive to SLR compared with harbour banks. For example, by 2130 the P5% ASCE for Purau varies by up to 10 m depending on the amount of SLR, whereas the 2130 P5% along the harbour banks only varies by up to 6 m under different SLR scenarios. For Charteris Bay and Hays Bay which are very low-lying, the maximum erosion extent, as a result of SLR, is assumed to be controlled by the height of the beach crest, so once the sea level exceeds the crest height and inundation occurs, there is no additional increase in erosion. This can be expected to occur beyond 1 m SLR.

The current and future P5% around Lyttelton Port (Cell 31) is -15 m, which represents the immediate hazard if the structures around the Port were to fail. As the shoreline around the Port is predominately reclamation fill it is it is likely structure failure without repair, would eventually result in the shoreline retreating to its ‘original’ natural position, however modelling this scenario was not within the scope of this study.

Table 5.5: ASCE widths (m) for the P66% ('likely') and P5% ('very unlikely') ASCE around the detailed sites in Lyttelton Harbour

Site	Cell	Probability of exceedance	Current	2050		2080			2130					
			0 m SLR	0.2 m SLR	0.4 m SLR	0.4 m SLR	0.6 m SLR	0.8 m SLR	0.4 m SLR	0.6 m SLR	0.8 m SLR	1 m SLR	1.2 m SLR	1.5 m SLR
Lyttelton Port	31	P66%	-12	-12	-12	-12	-12	-12	-12	-12	-12	-12	-12	-12
		P5%	-15	-15	-15	-15	-15	-15	-15	-15	-15	-15	-15	-15
Corsair Bay	32	P66%	-6	-7	-8	-9	-9	-9	-10	-10	-11	-11	-11	-12
		P5%	-8	-10	-11	-13	-14	-14	-15	-16	-17	-19	-19	-21
Cass Bay (east)	33	P66%	-19	-21	-21	-22	-23	-23	-23	-24	-24	-25	-25	-26
		P5%	-25	-27	-27	-29	-30	-30	-31	-32	-33	-34	-35	-36
Cass Bay (west)	34	P66%	-7	-8	-9	-10	-10	-10	-10	-11	-12	-12	-12	-13
		P5%	-9	-11	-12	-14	-15	-15	-16	-17	-18	-19	-20	-22
Rapaki Bay (east)	35	P66%	-3	-5	-5	-6	-6	-6	-7	-7	-8	-8	-8	-9
		P5%	-4	-6	-7	-9	-10	-11	-12	-13	-14	-15	-16	-17
Rapaki Bay (west)	36	P66%	-12	-13	-13	-14	-15	-15	-15	-16	-16	-17	-17	-18
		P5%	-15	-17	-17	-19	-20	-21	-21	-22	-24	-25	-25	-27
Charteris Bay (west)	42	P66%	-4	-10	-12	-15	-18	-20	-19	-22	-24	-25	-25	-25
		P5%	-6	-12	-15	-19	-22	-24	-26	-29	-31	-32	-32	-32
Charteris Bay (east)	43	P66%	-5	-6	-7	-7	-8	-8	-8	-9	-9	-10	-10	-11
		P5%	-7	-9	-10	-11	-12	-13	-14	-15	-16	-17	-18	-19
Hays Bay	44	P66%	-4	-8	-10	-11	-13	-13	-12	-14	-14	-14	-14	-14
		P5%	-6	-10	-12	-14	-16	-17	-16	-18	-19	-19	-19	-19
Purau	45	P66%	-4	-8	-10	-11	-14	-16	-12	-15	-17	-19	-20	-20
		P5%	-6	-10	-13	-14	-17	-20	-17	-19	-22	-24	-26	-27